5-2010

Synthesis of a directionally-conductive polyaniline hydrogel composite by vapor deposition.

Eric W. Reed 1987-
University of Louisville

SYNTHESIS OF A DIRECTIONALLY-CONDUCTIVE POLYANILINE HYDROGEL COMPOSITE BY VAPOR DEPOSITION

By

Eric W. Reed
B.S., University of Louisville, 2009

A Thesis
Submitted to the Faculty of the
University of Louisville
Speed Scientific School
as Partial Fulfillment of the Requirements
for the Professional Degree

MASTER OF ENGINEERING

Department of Chemical Engineering

May 2010

SYNTHESIS OF A DIRECTIONALLY-CONDUCTIVE POLYANILINE HYDROGEL COMPOSITE BY VAPOR DEPOSITION

Submitted by: _____
Eric W. Reed

A Thesis Approved on

_____

By the Following Reading and Examination Committee:

_____
Dr. Cindy K. Harnett

_____
Dr. Gerold A. Willing

_____
Dr. James C. Watters

ACKNOWLEDGMENTS

I would like to thank Dr. Gerold Willing for the opportunity to work in his research group and his time and patience, James Lee for his assistance in introducing me to his research, and Rodica McCoy and Dr. Jacek Jacinski at the Institute for Advanced Materials and Renewable Energy (IAM-RE) for training and usage of their equipment.

Thank you to the members of the Reading and Examination Committee: Dr. Cindy Harnett, Dr. Gerold Willing, and Dr. James Watters.

ABSTRACT

Electroactive polymers (EAPs), including conducting polymers (CPs) such as polyaniline (PAn), and hydrogels are exciting areas of research in disciplines such as biomedical engineering, with the goal of creating low-cost, lightweight, non-toxic artificial muscles with characteristics similar to natural muscle. Such a material could be used to create more natural prosthetic limbs or artificial heart muscle, which could be implanted in the left ventricle to assist patients with congestive heart failure. Currently, however, electroactive polymers are not a viable replacement for natural muscles for a variety of reasons, including insufficient applied force and lack of robustness [1]. Hydrogels suffer from many of the same limitations [2].

Electroactive polymers include conducting polymers (CPs) such as polyaniline (PAn), which has the general structure $[(\text{-B-NH-B-NH})_y(\text{-B-N=Q=N})_{1-y}]_x$, where B is a C_6H_4 ring in the benzene-like arrangement and Q is the same ring in the quinone-like arrangement. The 50% oxidized form, which is the most conductive, is termed emeraldine (y=0.5). Polyaniline is currently used in anti-corrosive coating and static-dissipating compounds, and has been proposed for use in electrochromic windows, flexible circuit boards, and conductive fabrics. Many research groups have developed methods for creating novel polyaniline structures and composites. However, the processibility of polyaniline is currently poor, and further work needs to be done before polyaniline or its composites can be considered viable artificial muscles [3].

This thesis describes a novel and exciting method for the creation of a patterned polyaniline-hydrogel composite which shows directional conductivity, a material which

has not been reported in the literature as far as we are aware. This material could provide the foundation for a micro- or nano-patterned composite which would further the goals of developing a viable artificial muscle with a directed pattern of contraction.

TABLE OF CONTENTS

NOMENCLATURE

A	Cross-sectional area of the sample
C_n	Flory characteristic ratio
D	Self-diffusion rate of water, 2×10^{-5} cm$^2 \cdot$ s^{-1} at 20°C
F	Free energy of swollen hydrogel
ΔF_{el}	Elastic free energy of swollen hydrogel
ΔF_m	Free energy of mixing of swollen hydrogel system
G	Elastic modulus of swollen hydrogel
G_0	Elastic modulus of unswollen hydrogel
h	Hydrogel sample thickness
I	Current
k_b	Boltzmann constant, 1.38×10^{-23} J $\cdot$ K^{-1}
l	Distance between current-carrying electrodes
$\overline{M}_c$	Molecular weight of hydrogel between crosslinks
$\overline{M}_n$	Number average molecular weight
M_r	Molecular weight of repeat unit
$\overline{M}_w$	Weight average molecular weight
n_s	Number of solvent molecules in swollen hydrogel
R	Resistance
R	Universal gas constant, 8.314 J $\cdot$ mol^{-1} $\cdot$ K^{-1}
$\overline{r}_0$	Root mean square distance of polymer chains between neighboring crosslinks
T	Absolute temperature
t	Diffusion time
V_p	Volume of dry hydrogel
$\tilde{V}_S$	Molar volume of solvent
V	Voltage
V	Volume of swollen hydrogel
w	Sample width

Greek Symbols

α	Linear deformation factor
κ	Fraction of active network parameter
μ_S	Chemical potential of solvent in swollen hydrogel
μ_S^o	Chemical potential of solvent in surrounding liquid
ν	Specific volume of hydrogel
v_e	Cross-link density
ξ	Correlation distance
ρ	Resistivity
ρ_P	Bulk polymer density
ρ_s	Surface resistivity
τ	Stress applied to hydrogel sample
$\mathbf{\Phi}_s$	Volume fraction of solvent in swollen hydrogel
$\mathbf{\Phi}_s^0$	Volume fraction of solvent in hydrogel as synthesized
χ	Flory-Huggins interaction parameter between solvent and polymer

LIST OF TABLES

LIST OF FIGURES

I. INTRODUCTION

A. Electroactive Polymers

Electroactive polymers (EAPs) have been a growing area of research over the past decade. Like electroactive ceramics and shape memory alloys, EAPs respond to electrical stimuli with a displacement of the material, which can create usable force. Unlike older materials, EAPs can apply greater induced strains, have faster response times, and are less dense and more resilient. However, EAPs currently can only apply small forces, have a low mechanical energy density, and are not robust enough for many commercial applications [1].

Electroactive polymers can be divided into electronic electroactive polymers, which are driven by electrical fields or Coulomb forces, and ionic electroactive polymers, which involve ion mobility and diffusion. Electronic EAPs include ferroelectric polymers, which work on the principle of piezoelectricity, and dielectric polymers. Ionic EAPs include ionic gels, ionomeric polymer-metal composites (IPMC), and conductive polymers. In general, ionic EAPs require lower voltages than electronic EAPs and provide bending actuation with large amounts of deflection, although extensional mechanisms can be constructed. Their direction of bending also relies on the polarity of the applied voltage, so that a component made with an ionic EAP is inherently bidirectional. However, ionic EAPs have slow response times (fractions of a second to seconds, compared to 40 milliseconds for human leg muscle [74]), provide a relatively small amount of force when bending, require an electrolyte and a method of enclosure if

operating in an open-air environment, require expensive gold or platinum electrodes to carry high currents, and cause hydrolysis in aqueous systems at applied voltages above 1.23 V [1, 4].

Conductive polymers include polypyrrole, polythiophenes, and polyaniline function via reversible doping and dedoping that occur during redox reactions. A sandwich consisting of an electrolyte between two conductive polymer electrodes forms a simple actuator. When a voltage is applied, hydrogen ions diffuse into one polymer electrode, causing swelling, and diffuse out of the other polymer electrode, causing shrinkage. The combination of these two changes in volume causes the device to bend. Thinner electrodes result in faster response times but have a smaller induced force. Conductive polymers have attractive properties, such as electrical properties similar to those of metals or semiconductors, while offering the ease of synthesis and processing of polymers. These properties have led to the usage of conductive polymers in microelectronic devices such as batteries, light emitting diodes, electrochromic displays, and micro-electro-mechanical systems (MEMS) [5, 6]. Unfortunately, conductive polymers generally require 1-5 V for actuation, and have relatively high energy densities (20 J/cm^3) but low efficiencies (1%) [1].

B. Conductivity

The ability of a material to pass current is known as its conductivity. Conductivity is the inverse of resistivity, ρ , and thus conductivity has the units of inverse ohms, which

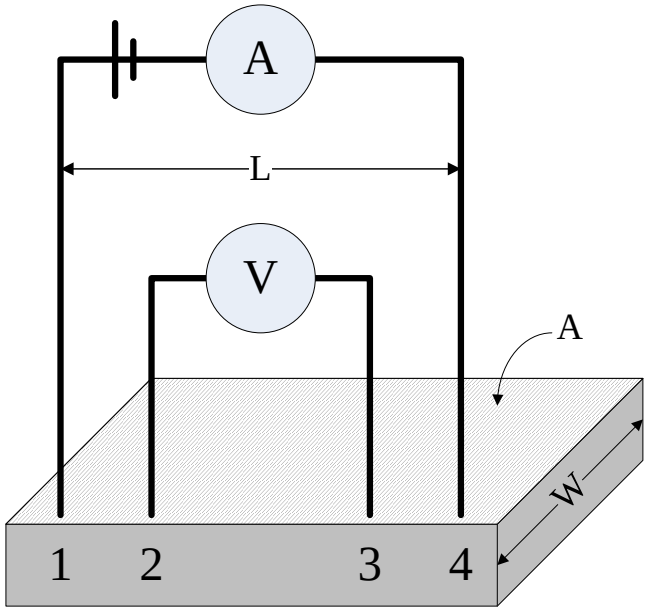

Figure 1. Schematic of a four-point probe measurement. Current is applied to the sample across connections 1 and 4. The voltage is measured between connections 2 and 3. Based on [7].

are termed Siemens (S). Insulators are generally considered to have conductivities of less than 10^{-8} S/cm, while conductors have conductivities of greater than 10^{3} S/cm. Semiconductors have intermediate conductivities. Resistivity is determined experimentally by measuring a material's resistance (R), usually using the four-point probe technique.

The four point probe technique involves applying a current I between two electrodes placed on the surface of a material and measuring the potential difference V between another pair of electrodes (Figure 1). R can be calculated using Ohm's Law which can then be used to calculate resistivity:

$$\rho = \frac{RA}{l} \tag{1}$$

$$\rho_s = \frac{Rw}{l} \tag{2}$$

Here, ρ is the bulk or volume resistivity, ρ_s is the surface resistivity, R is the sheet or surface resistivity, sometimes denoted as R_s, A is the cross-sectional area of the sample, l is the distance between the current-carrying electrodes and w is the sample width. These equations hold only for square or rectangular samples where the thickness of the sample is much less than the spacing of the four-point electrodes. Surface resistivity does not take into account the thickness of the sample, while bulk conductivity does. For a square sample, surface resistivity equals surface resistance, which is given the units Ω /square (to distinguish it from resistance, "square" is dimensionless). Bulk resistivity can be converted to resistance in Ω /square by dividing by the sample thickness [5].

C. Conductive Polymers in Biomedical Applications

Conductive polymers have been investigated for biomedical applications since the 1980s, when it was discovered that they were compatible with many biological molecules. In the 1990s, it was shown that via electrical stimulation, conducting polymers were able to regulate cellular activity including DNA synthesis and protein secretion, specifically in cells such as nerve and cardiac cells which respond to electrical stimuli. Conducting polymers can undergo reversible doping, can transfer charges to biochemical reactions, and potentially can be modified for specific applications. Some potential biomedical applications include biosensors, tissue scaffolds, drug delivery devices and actuators. In biomedical applications, conducting polymers have advantages over traditional metallic or semiconductive devices: they are less expensive, easier to

synthesize, more versatile, and can have surface areas fifty times as large as standard metallic electrodes [5].

Currently, conducting polymers are the materials which most closely mimic the properties of biological muscles [8]. For this reason, electroactive polymers have been proposed as artificial muscles, which researchers hope will soon be comparable to biological muscles in strength and durability. Conductive polymers have been used to create actuators for biomimetic robots as well as gripping and lifting devices for spaceflight applications with the hope that a prosthetic arm utilizing electroactive polymers will soon be developed [9]. Other reported devices include focus controls for small camera lenses, audio speakers and active diaphragms for pumps [8]. Conducting polymers are also being investigated as chemical and biological sensors. So far, conducting polymers have been synthesized for or suggested as pH sensors and sensors for inorganic ions, organic molecules, and gases. They have also been used as chemical noses or tongues for fields from food science to soil and wastewater analysis [10].

Chemical polymerization of conducting polymers allows large-scale production techniques and post-polymerization modifications of the structure. Unfortunately, thin films cannot be created by this method. It is easy to create thin films with electrochemical polymerization, though there can be some difficulty in removal from the electrode [5]. Electrochemical polymerization is often conducted in a three electrode cell (Figure 2). A solution of monomer in solvent is placed in the cell and a potential difference is applied between the working and counter electrodes (measured against the reference electrode).

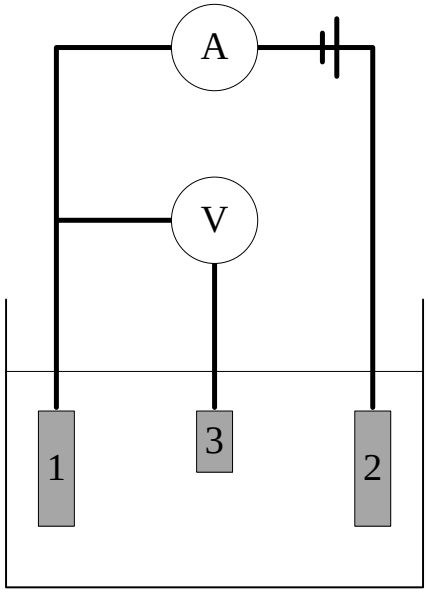

Figure 2. Schematic of a standard three electrode cell used for electropolymerization. 1 is the working electrode, 2 is the counter electrode, and 3 is the reference electrode. Based on [11].

Some of the future challenges facing the field of electroactive polymers include mechanical characterization, improving cyclic response, and modeling of mechanical properties [3]. Electroactive polymers currently exhibit low applied forces and low efficiencies, and are not robust enough for continuous usage. Additionally, there is no overarching analysis of phenomena involved in activation. Adequate understanding of the response, properties, and processing relationship needs to be established so that basic chemistry and analytical tools can be used to EAP behavior such as actuation force [1]. Currently, the processability of many conducting polymers, including polyaniline, is poor [12-14]. However, in 2006, Artificial Muscle, Inc. launched the first commercial line of linear actuators based on conducting polymers [15]. After an initial global market of $15 million in 2007, the market for devices based on electroactive polymers is expected to increase to $247 million by 2012 [16].

To further develop these materials, reproducible synthesis, fabrication, and processing techniques need to be established and refined. Reliable tests for response characteristics need to be developed, so that a comprehensive database of material properties can be constructed. Various devices and configurations will need to be tested and optimized prior to full commercialization. Because these challenges cut across a number of the traditional boundaries between fields, interdisciplinary teams and international cooperation are needed for the further development of EAPs [1].

D. Polyaniline

Polyaniline (PAN, PAni) conducts electricity via a process of partial oxidation and reduction. It has the general structure of $[(\text{-B-NH-B-NH})_y(\text{-B-N=Q=N})_{1-y}]_x$, where B is a C_6H_4 ring in the benzene-like arrangement and Q is the same ring in the quinone-like arrangement (Figure 3). The fully oxidized form is known as pernigraniline (y=0), while the fully reduced form is called leucoemeraldine (y=1). The 50% oxidized form is termed emeraldine (y=0.5) [17]. Polyaniline is stable to both air and moisture in both its conductive doped form and insulating de-doped form, which makes it one of the most useful conducting polymers. It also has a very simple doping/dedoping reaction (Figure 4) [18]. This doping reaction is facile and occurs under moderate conditions, due to the presence of the basic nitrogen heteroatom in the backbone chain [19]. The doped emeraldine salt phase appears as a deep green color, while the de-doped emeraldine base phase appears as a dark blue color [20]. The chemical synthesis of polyaniline frequently involves free-radical polymerization, usually using an initiator such as ammonium

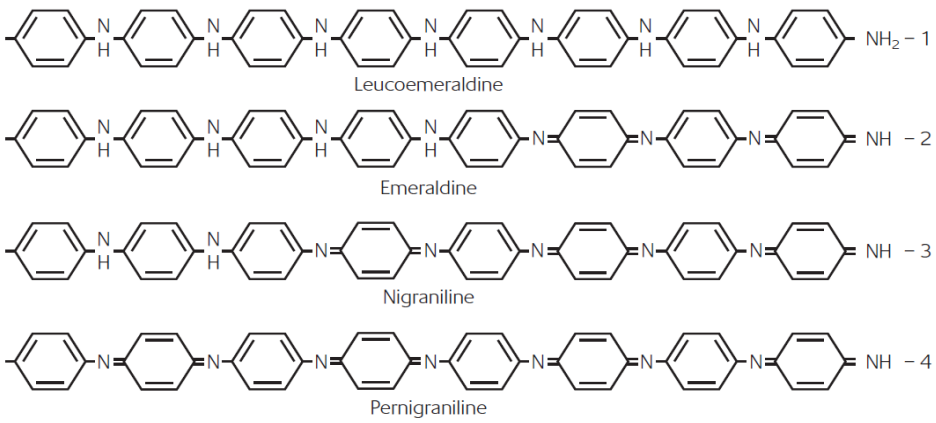

Figure 3. Oxidation states of polyaniline. From [21].

persulfate (Figure 5). This reaction is facile and proceeds under relatively mild conditions.

The conductivity of polyaniline can be adjusted by incorporating it into compounds or doping it with a secondary agent. Polyaniline can easily be mixed with other types of polymers, which has led to its use in static-electric dissipating compounds and anti-corrosion coatings [14, 17]. Specifically, it is hoped that electroactive polymers will enable low-cost electronic devices such as organic light-emitting diodes (OLEDs) and solar cells. It has been proposed for future usage in electrochromic windows, flexible circuit boards, and conductive fabrics. Because of its many useful properties, as well as its ease of synthesis and volume of literature available on the subject, polyaniline was chosen to create the novel composite described in this work.

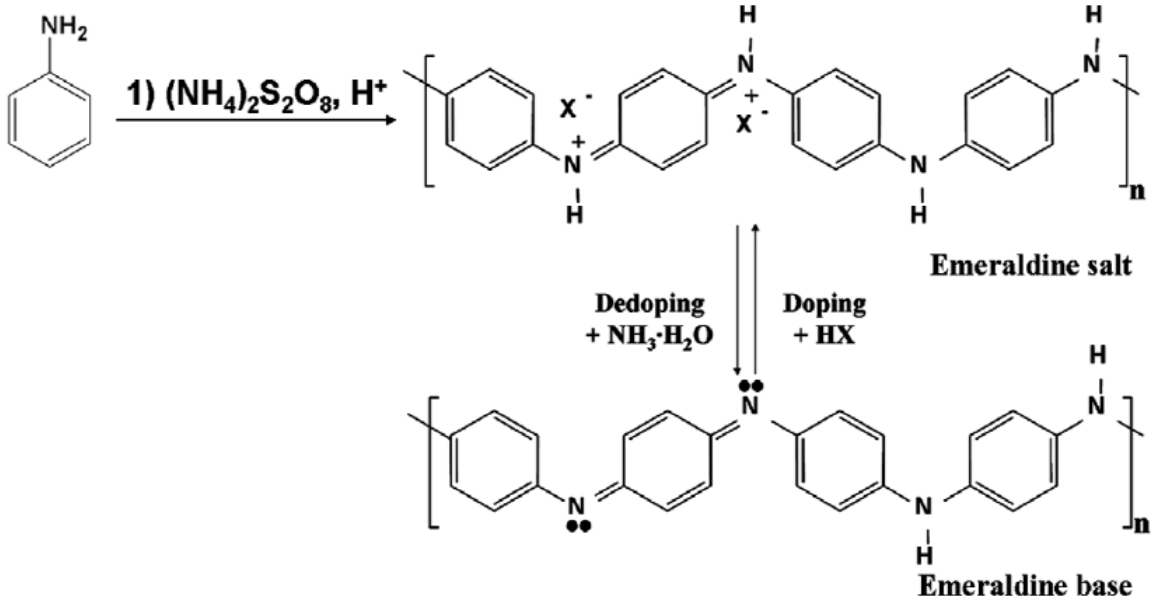

Figure 4. Polymerization and doping/dedoping reactions of polyaniline. From [18].

E. Polyaniline as Artificial Muscle

Polyaniline has been explored as a biocompatible, biodegradable scaffold for tissue engineering purposes as well as a bioactuator or "artificial muscle". Compared to traditional artificial muscles, polyaniline is lightweight, inherently biocompatible, and works in the natural conditions present in the human body. Unfortunately, at present, it is subject to delamination and its response time is limited by ion mobility. Modification techniques have included adsorption or entrapment of molecules, covalent modification of the polymer structure, and micro- or nano-scale patterning of the polymer surface [5].

Polyaniline has been used to create artificial muscles which operate via a bending mechanism (Figure 6). They function either in solution or in free space via an applied voltage of 1.5 V without generation of gases in solution [22]. Herod and Schlenoff studied the expansion and contraction behavior of polyaniline films under tension exposed to both chemical and electrochemical doping/dedoping reactions. They found

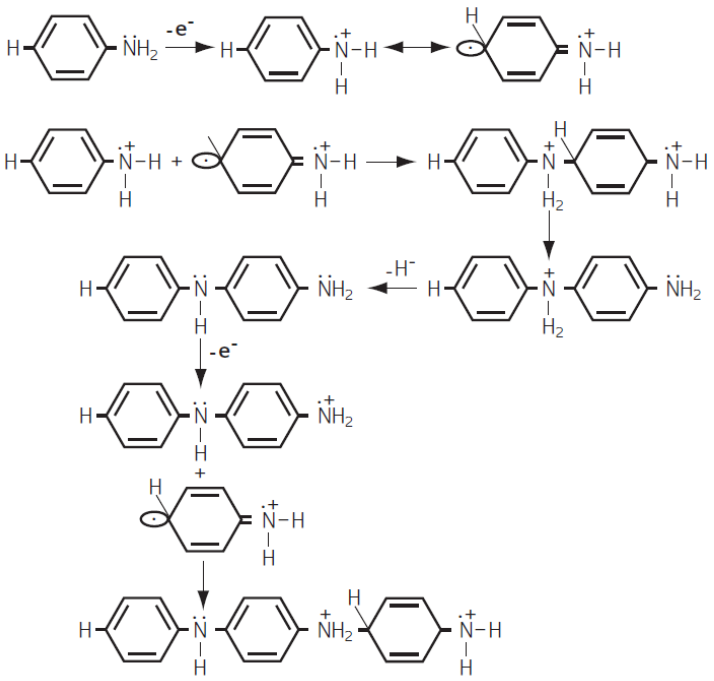

Figure 5. Mechanism for the free-radical polymerization of aniline. From [17].

strongly anisotropic expansion when dedoped drawn polyaniline was exposed to different protonic acids. Polyaniline films with randomly-oriented chains showed extensions of 7% when exposed to aqueous HCl, and films with aligned chains showed extensions of 11% in the direction parallel to the alignment. Electrochemical doping and dedoping by passing current through polyaniline films in aqueous H_2SO_4 resulted in reversible changes in the length of the films. Unlike chemical doping, films with chains oriented perpendicular to the direction of tension showed the highest elongation. These films also exhibited a significant amount of "creep", that is, a residual amount of elongation even when fully dedoped [19].

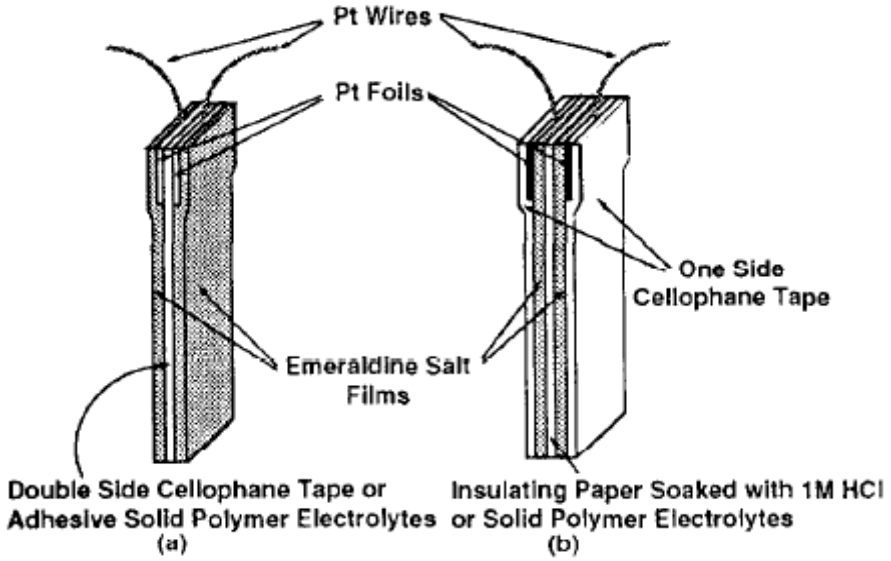

Figure 6. Polyaniline artificial muscles created by Kaneto et al. (a) "Backbone type" actuator. (b) "Shell type" actuator. From [22].

F. Nanocomposites

Polymeric nanocomposites incorporate nanometer-scale particles into polymers in an attempt to increase properties such as conductivity. These composites also have the advantage of having adjustable properties depending on the nanoparticle concentration [12]. The nanoparticles can be distributed in a preformed bulk polymer by mixing; however, the nanoparticles tend to agglomerate during this process. More recent approaches attempt to create the nanoparticles during polymerization, thus assuring an even distribution [23]. Many composites of metals or metal oxides and conjugated conducting polymers have been fabricated.

Mallikarjuna et al. studied the addition of γ-Fe_2O_3 nanoparticles to polyaniline. They observed an increase in conductivity as the percentage of nanoparticles in the composite increased, which they attributed to the ferromagnetic nature of γ-Fe_2O_3 [12].

Neelgund et al. developed a one-step procedure for the incorporation of silver particles into polyaniline and polyaniline derivatives, and reported a uniform dispersion of nanoparticles within the bulk polymer [23]. Cho and Park dispersed platinum, silver, and gold nanoparticles onto thin films of conducting polymers, including polyaniline, and confirmed that electrical contact was being made between the polymer and the included nanoparticles via current-sensing atomic force microscopy [24]. Nanocomposites using hydrogels have also been synthesized [25].

G. Biological Impact of Aniline

IARC lists aniline as a Group 3 carcinogen ("not classifiable as to its carcinogenicity in humans") due to inadequate evidence of carcinogenicity in humans, and limited evidence in animals. The incidence of bladder cancers in workers in the aniline-dye industry have generally been attributed to chemicals other than aniline [26]. However, the US EPA lists aniline as a Group 2B carcinogen ("probable human carcinogen") due to "sufficient" evidence of carcinogenicity in animals, but "inadequate" evidence in humans. Two different strains of rats showed increases in tumors of the spleen and body cavity when exposed to doses of aniline up to 6,000 ppm [27].

Polyaniline is known to be biocompatible; however, it is unknown if the residual amount of monomers or initiators remaining in the system will be harmful to human cells. The author is unaware of any studies in which polyaniline has been shown to be toxic, and at least one study implanted polyaniline films subcutaneously into rats with no visible adverse effects [28]. Further studies will need to be conducted in this area.

H. Gold and Gold Nanocomposites

Gold is frequently chosen as a material for creating nanocomposites due to its biocompatibility and its ability to increase the conductivity of the material forming the composite. For example, Granot et al. found that a polyaniline system containing gold nanoparticles had a charge transport enhanced 25 times that of an equivalent system containing poly(4-styrene-sulfonate) [29]. The addition of only 0.2% by weight of gold nanoparticles to poly(methyl methacrylate) was observed to decrease the resistivity of the system by 40% [30]. The conductivity of the composite may change depending on the size, distribution, and alignment of the nanoparticles. Aligned nanorods or nanowires may decrease the tortuosity of the path of electrons through the material even further.

The incorporation of gold nanoparticles into polyaniline leads to a composite with different properties than either of its components. Gold-polyaniline composites were pioneered by E. T. Kang and coworkers in 1993, and have been expounded upon since then. Hydrogen peroxide, ammonium persulfate (APS), and tetrachloroauric acid ($HAuCl_4$) have all been used to initiate the polymerization of polyaniline. Several of the synthesis techniques are described *vide infra*. Mechanistically, the synthesis of polyaniline with APS is well known, while synthesis using the tetrachloroaurate ion is more complex; however, one-step syntheses of gold-polyaniline composites are possible. There is currently a great deal of scientific interest in gold-polyaniline composites, since they have novel properties which can be altered by morphology and synthesis techniques. It is hoped that they will lead to breakthroughs in materials science [17]. Gold nanoparticles may also be used to create micro-electro-mechanical systems (MEMS).

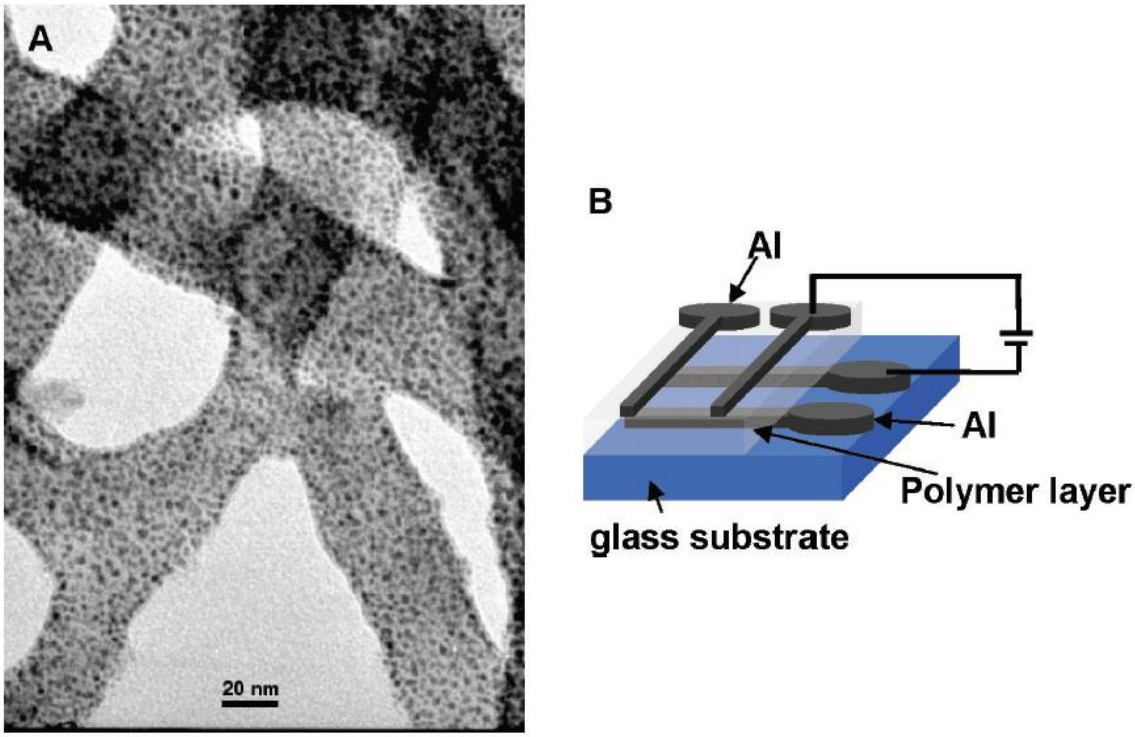

Figure 7. (a) Transmission electron micrograph (TEM) of a polyaniline nanofiber studded with gold nanoparticles. (b) The construction of a nonvolatile memory device fabricated from this composite. From [31].

Tseng et al. created a nonvolatile memory device from 30-nm polyaniline nanofibers decorated with 1-nm gold nanospheres with a 3-order-of-magnitude difference in conductivity between the "on" and "off" states (Figure 7) [31]. A review of recent gold-polyaniline nanocomposites has been published [32].

I. Hydrogels

Hydrogels are cross-linked polymers with hydrophilic groups which can change volume by absorbing water or other solutes in a process called swelling. The amount of swelling is dependent both on the properties of the polymer matrix and the environmental conditions such as temperature. The swelling behavior of hydrogels is one of their most

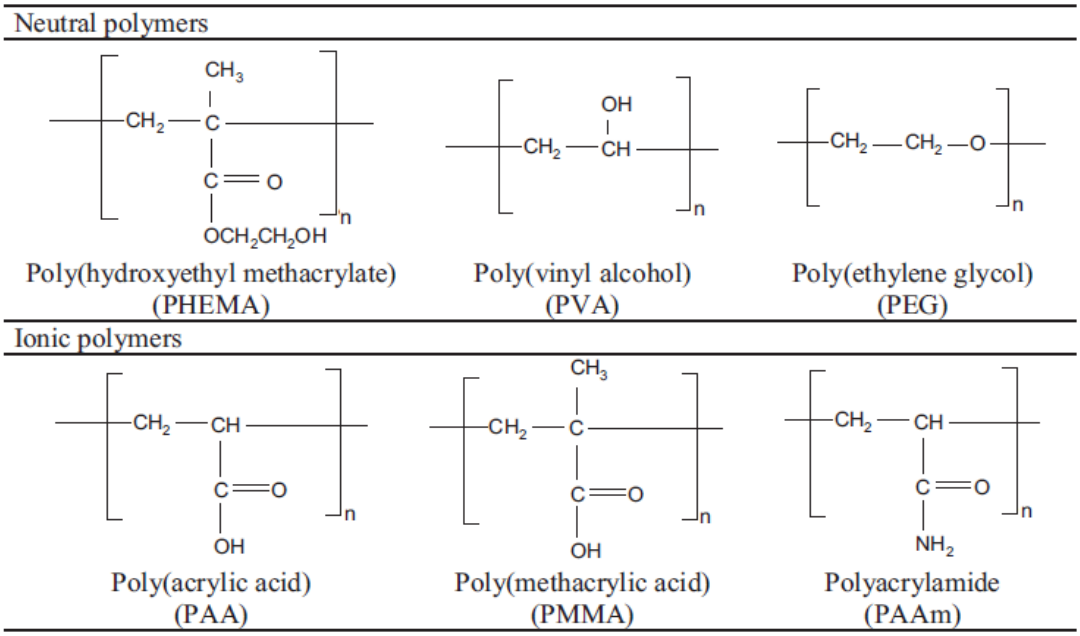

Figure 8. The chemical structures of a variety of hydrogel materials being studied for biological and medical applications. From [33].

important properties. The degree of swelling can be expressed as [34]:

$$q = \frac{m_{gel}}{m_{gel\,(dry)}} \tag{3}$$

Hydrogels are found widely both in nature, as in animal and plant tissues, and in industry, as in controlled drug-release devices [33, 35] and soft contact lenses [34]. They have been considered for applications such as biosensors, microfluidic devices, and tissue implants and engineering [33, 36]. Peppas et al. have written a review of the application of hydrogels to biomedical applications [33]. The structure of a variety of hydrogel materials can be seen in Figure 8.

The performance and properties of a hydrogel depend to a large extent on its bulk properties, such as volume fraction of the gel in its swollen state (v_N), the molecular weight between crosslinks ($\overline{M}_c$), and the corresponding mesh size (ξ). The structure of non-ionic hydrogels can be described by the Flory-Rehner model [33]. The Flory model

assumes that the free energy of the polymer is the sum of the free energy of the mixing and the elastic free energy

$$\Delta F = \Delta F_{el} + \Delta F_m \tag{4}$$

which is a reasonable assumption at all but the highest cross-linking densities. The elastic free energy can be written as

$$\frac{\Delta F_{el}}{k_b T} = \kappa \left(\frac{V_p \nu_e}{2}\right) \sum_{i=1}^{3} (\alpha_i^2 - 1 - \ln \alpha_i) \tag{5}$$

where α , the linear deformation factor, is defined as

$$\alpha = \left(\frac{V}{V_p}\right)^{\frac{1}{3}} \tag{6}$$

and ν_e , the cross-link density, can be written as

$$\nu_e = \frac{\rho_P}{\overline{M_c}} \tag{7}$$

where V is the volume of the swollen polymer, V_p is the volume of dry polymer, k_b is the Boltzmann constant, T is the absolute temperature, ρ_P is the density of the bulk polymer, and the fraction of active network κ is a fitting parameter between 0 and 1 which accounts for imperfections in the polymer matrix.

The free energy of mixing includes contributions from both enthalpy and entropy terms:

$$\frac{\Delta F_m}{k_b T} = [n_S \ln(1 - \Phi_s) + \chi n_s \Phi_s] \tag{8}$$

Here n_s is the number of solvent molecules, Φ_s is the volume fraction of the polymer matrix in the swollen gel, and χ is the Flory-Huggins interaction parameter between the solvent and the polymer matrix. If the network is isotropic, the linear expansion α is the same in all three directions. If this is the case, then the swelling equilibrium of the

chemical potentials of the solvent in the gel, μ_S, and in the surrounding liquid, μ_S^o, can be written as

$$\mu_S - \mu_S^o = \left[\frac{\delta}{\delta n_S}\left(\frac{\Delta F}{k_b T}\right)\right]_{T,P} = [\ln(1-\Phi_s) + \Phi_s + \chi\Phi_s^2] + \kappa\rho_P\tilde{V}_S M_c^{-1}\left(\Phi_s^{1/3} - \frac{\Phi_s}{2}\right) = 0 \quad (9$$

where $\tilde{V}_S$ is the molar volume of the solvent [37]. Using the theory of rubbery elasticity, and accounting for the volume fraction density of the chains during crosslinking, the molecular weight between crosslinks can be written as

$$\frac{1}{\overline{M}_c} = \frac{2}{\overline{M}_n} - \frac{\frac{\nu}{\tilde{V}_S[\ln(1-\Phi_s) + \Phi_s + \chi(\Phi_s)^2]}}{\Phi_s^0\left[\left(\frac{\Phi_s}{\Phi_s^0}\right)^{\frac{1}{3}} - \left(\frac{\Phi_s}{2\Phi_s^0}\right)\right]} \quad (10)$$

where Φ_s^0 is the volume fraction of the solvent in the gel as synthesized and ν is the specific volume of the polymer [33].

This analysis becomes more difficult for a system containing ions. Maurer and Prausnitz give equations for systems containing ionic species, as well as for polyelectrolyte gels both without and with common ions [38].

For simple systems of hydrogels with relatively small deformations (<20%), $\overline{M}_c$ can be experimentally determined if the hydrogel is assumed to follow the rubber elasticity theory by applying stress to a polymer sample:

$$\tau = \frac{\rho_P RT}{\overline{M}_c}\left(1 - \frac{2\overline{M}_c}{\overline{M}_n}\right)\left(\alpha - \frac{1}{\alpha^2}\right)\left(\frac{\Phi_s}{\Phi_s^0}\right)^{\frac{1}{3}} \quad (11)$$

One method of describing the pore size of a hydrogel is by the correlation length, ξ. This is defined as the straight-line distance between crosslinks and is calculated as

$$\xi = \alpha(\bar{r}_0^2)^{\frac{1}{2}} \quad (12)$$

where $\bar{r}_0$ is the root mean square distance of polymer chains between neighboring crosslinks. If the hydrogel swells isotropically, then

$$\alpha = \Phi_s^{-\frac{1}{3}} \tag{13}$$

and the correlation distance can be written as

$$\xi = \Phi_s^{-\frac{1}{3}} \left(\frac{2C_n \bar{M}_c}{M_r} \right) \tag{14}$$

where C_n is the Flory characteristic ratio and M_r is the molecular weight of a repeat unit. The ability of these properties to be adjusted to customize mechanical, responsive, and diffusive characteristics makes hydrogels attractive for biological and medical applications [33].

Responsive hydrogels have properties such that they respond to specific changes in their environment, such as pH, temperature, or ionic strength of the liquid surrounding the hydrogel. Composites can be formed by the incorporation of micro- or nano-scale materials into the polymer matrix. These composites have properties such that their swelling behavior can be controlled by stimuli over a distance, such as by light or an applied magnetic field [36].

J. Hydrogel Actuators

Polymer hydrogels have been suggested as artificial actuators for biomedical purposes. Biological muscles have a developed stress of over 300 kPa, linear contractions of 25%, and response times of fractions of a second, and currently serve as the benchmark for artificial muscles. Natural muscles are powered by the hydrolysis of

adenosine triphosphate (ATP) to adenosine diphosphate (ADP) and a free phosphate, which powers the actin-myosin muscle system. By analogy, it has been theorized that hydrogels should be able to act as muscles, but this comparison makes matters deceptively simple, while in practice they are much more difficult.

Polymer hydrogels function by a change in volume, which is necessarily rate-limited by the diffusion of water or solvent into or out of the bulk gel. The maximum force that can be developed is also limited by the change in free energy of the system caused by the change in solvent content. However, natural muscle is a chemically-driven system, which operates via the cyclic conformation change in myosin which causes it to "walk" along actin fibers. It uses a very potent energy source (the dephosphorylation of ATP), and only generates force when ATP is consumed, rather than proceeding between two states as hydrogels do.

A gel must be stiff enough to exert a desired force and strong enough to bear the load desired to be moved in order to be useful as an actuator. It also must have a short diffusion time if it is actuated by swelling behavior. Since gels are difficult to mold after synthesis, it must be possible to synthesize the gel in a suitable shape by *in situ* polymerization. Currently, most gels are used in applications such as food or pharmaceuticals where mechanical robustness is not needed. If natural muscle is used as a target, the hydrogel used should have a fracture strength of at least 1 MPa and an elastic modulus greater than 12 MPa, to prevent the active contraction from being cancelled by passive contraction under a load. Gels with lower applied forces may be useful for applications such as microfluidics valves. Elastic modulus represents the rigidity under

stress, while tensile strength is the ability of a material to withstand a static load without cracking or permanently deforming.

There are many examples of hydrogels in the natural world, such as seaweed or the bodies of marine invertebrates such as sea anemones. Human cartilage, the cornea of the eye, the dermis and arterial walls are all gels reinforced with fibers. These tissues need to operate in environments with large reversible strains and be able to withstand substantial impacts without damage. The stress-strain curve of such a material is very non-linear and its properties at very high strains become important. This is in stark opposition to more traditional materials such as metals or ceramics, which have largely linear stress-strain curves up to about 1%, where yield or fracture occurs. These properties are more reminiscent of rubbery materials, which are less common in structural engineering applications. Currently, there is not a large literature database on the mechanical properties of simple gels.

To understand the elastic modulus of a gel, it can be viewed essentially as a diluted rubber, since polymers above their glass transition temperatures are free to experience large-scale molecular motion, and a gel can be viewed as a cross-linked solution. The elastic moduli of gels are relatively small (less than 10 MPa) and decreases as the fraction of solvent in the gel increases. For example, gelatin swollen to five times its dry weight has an elastic modulus of 800 kPa and a fracture stress of 70 kPa. When swollen to 40 times its dry weight, it has an elastic modulus of 40 kPa and a fracture stress of 6 kPa. The elastic modulus of a hydrogel can be modeled as

$$G = A\frac{\rho}{M_c}RT(\Phi_s^0)^{\frac{2}{3}}(\Phi_s)^{\frac{1}{3}} \tag{15}$$

Thus the modulus compared to the initial value as a function of swelling can be described as

$$\frac{G}{G_0} = \left(\frac{\Phi_s}{\Phi_s^0}\right)^{\frac{1}{3}} \quad (16)$$

Currently, synthetic gels are much too weak to be used in structural applications. Natural gels are much stronger, probably due to the presence of microstructures which synthetic gels lack. In testing the strength of a hydrogel sample, several factors must be taken into account which can be ignored in denser materials such as metals. For example, since gels fracture at much higher strains than metals or ceramic materials, the time dependence of their behavior must be taken into account. Depending on whether the gel samples are tested in air or submerged in solvent, water may be taken up or lost during the course of the test. At high compressive strains, sample geometry can result in high shear stresses of the polymer sample against the plates of the testing apparatus, which can put the sample into hydrostatic compression where failure never occurs. However, based on these equations, it can be shown that current hydrogels can generate substantial forces. For example, a gel with 50% water content and an elastic modulus of about 1 MPa, similar to a contact lens, could generate a stress of 165 kPa with a change in thickness from 50% greater than its original thickness to 25% greater.

Most rigid amorphous polymers exhibit brittle facture under tension. Elastomers, since they are essentially liquid polymers, do not undergo crazing (void formation) and so do not exhibit brittle fracture behavior. Their fracture behavior is not explained by the Griffith model, because most of the energy involved is used stretching individual polymer chains across the fracture point rather than crazing. Unreinforced elastomers readily tear at any cut due to a lack of energy-absorbing mechanisms.

Similarly, the properties of unstructured gels are analogous to rubbers. The strength of a gel can be related to the strength of a rubber with the same cross-link density by accounting for factors such as the dilution of the gel network and extension of the polymer chains by the solvent. Some rubbers do exhibit energy-absorbing mechanisms, such as crystallization at high tensile stresses or large fracture energies in tire rubber, when diene chains slip over the surface of carbon black particles. Natural gels such as agarose exhibit regions of helices which help reinforce their structure. As could be expected, the properties of these gels depend on the amount of structure developed during gel formation. It may be possible to reinforce synthetic gels, which currently lack such structures, to increase their mechanical properties. One such application of the mechanical properties of gels has been in research for contact lens materials, where there is no benchmark for what determines strength and there is no simple relationship between water content or polymer structure and gel strength.

Most gels form in two-phase systems, consisting of polymer-rich and polymer-poor regions. Synthetic and natural gels apparently consist of crystalline areas separated by areas of solubilized polymer chains. Various attempts have been made to increase the strength of synthetic gels by altering the nanostructure of the gel, such as freeze-thaw cycling, irradiation, and addition of plates or fibers, as is seen in natural collagen. Because hydrogels have the ability to take up and release small molecules, they can be used as sensors. Measurements of the diffusion coefficients of small molecules in swollen hydrogels reveal that their diffusivities do not differ greatly from their diffusivities in pure solvents. However, when a polymer gel becomes swollen or shrunken by the diffusion process, there is a significant difference in the mechanism of the diffusion.

Large non-uniform changes in volume cause highly non-Fickian behavior and may cause significant internal stresses. In a single-phase gel, the diffusion and solubility of a solute will change over the course of the process. In two-phase gel systems, the problem becomes even more complex.

In building a gel-based actuator, it is important that swelling behavior occurs only over a range where surface properties are constant, meaning that sample size, diffusion rate, and response time are coupled [2]. The self-diffusion rate of water at 20°C is approximately $D = 2 \times 10^{-5}$ cm^2/s [39], and diffusion times can estimated as

$$t = \frac{2h^2}{D} \tag{17}$$

where h is the thickness of the sample. Assuming a thickness of about one millimeter, this gives a response time of about one minute, which is the upper bound for the usefulness of these devices. Drying is also an issue with hydrogel-based devices. Unlike linear polymers, hydrogels are highly cross-linked and thus cannot be processed in a melt or solution phase after synthesis, so methods to polymerize hydrogels *in situ* must be used. Methods that allow construction of gels containing multiple layers and electrodes must also be developed. Most of the synthetic gels under investigation are formed by the free radical polymerization of acrylate monomers. These monomers tend to polymerize atactically, making the formation of strengthening microstructures limited [2]. Additionally, since oxygen is a free-radical scavenger [40], control of the polymerization can be difficult and can lead to irreproducible results, especially in small scale syntheses. Characterization of the resulting hydrogels can be difficult due to their network cross-linked structure. Reproducible samples can be synthesized by irradiating a degassed reaction mixture held between glass plates with ultraviolet (UV) light.

However, due to attenuation of the UV light, sample properties can change through the thickness of the sample, and unpolymerized chain ends may be present. Reaction kinetics determine the amount of solvent remaining in the mixture during polymerization, which effect the network structure and ability of the final product to swell. Good mechanical properties are obtained when hydrogels are less than 50% water at equilibrium, compared to the low-densely cross-linked hydrogels with large degrees of swelling which are commonly studied.

Polymers chains in solution change conformation in response to temperature changes. For this reason, there is a lower critical solution temperature (LCST) above which the hydrogel separates into polymer-rich and dilute phases. This behavior can be likened to the contraction of linear polymer coils under high stress and temperature conditions [41].

Gel swelling can be treated as a two-step process. In the first step, solvent diffuses into the gel and causes swelling. In the second step, there is an instantaneous conformation change to relieve the stress between swollen and unswollen regions. For one-phase gels involving a small volume change, diffusion behavior can be adequately modeled. For two-phase gels or those involving large volume changes, the kinetics of diffusion are complex [2].

The response time of a polymer system can be improved by increasing the porosity of the gel so that the diffusion distances are minimized. Macroporous hydrogels contain nano- to micrometer-sized channels in the bulk crosslinked polymer phase. The term “macroporous” denotes only that the pores are inherent in the material and do not arise from voids created by swelling behavior; it states nothing about pore size. One of

the simplest ways to synthesize a macroporous hydrogel is the inclusion of an inert material soluble in the monomer solution, followed by a phase separation during the polymerization reaction. Once the diluent is removed, pores or voids remain in the cross-linked polymer network [42].

The ability of a hydrogel to respond to its environment allows it to produce a force in response to a change in the chemistry around it, whether it is a change in pH or solvent. Alternatively, polyelectrolyte gels can be actuated by the application of electrical current to a solution, which causes pH changes near the cathode and anode. Depending on the positions of the electrodes, the gel can be made to move in a variety of ways. Typically, a thin strip of a gel will deflect in alternating directions as the sign of the potential difference across it is cycled. These devices show a quick response time and a large deflection, but the applied stress can be quite small. The elastic modulus of the hydrogel needs to be large enough that the blocking force, or force applied at the end of the actuator, is also large. The best polymeric actuators so far have developed a blocking force of 50 times their own weight; natural muscle in linear contraction delivers about 300 times its own weight in force. Hydrogels have achieved 135 J/kg of mechanical energy density but only 2 W/kg power density, as compared to 70 J/kg and 100 – 200 W/kg, respectively, for natural muscle, which has a power density similar to that of a lithium battery.

Thermal activation provides a convenient mechanism for driving actuators such as those made of poly(NIPAAm); however, cooling processes are slow at these low temperatures. A polymer with a higher LCST could undergo more rapid changes in temperature and thus be actuated more quickly. Heating and cooling equipment would

also add substantially to the weight of an article muscle used as an artificial limb, for example. Chemical activation is similarly attractive but would also require large amounts of piping for chemical transport. Electrical transport may be attractive in theory, but based on the number of ions needed to be transported into or out of a gel, the currents needed would be very large (>10 A). If the electrolysis reaction also produces gas, a removal mechanism will be needed. The electrodes themselves will also need to be able to flex with the gel, while not restricting the volume changes of the gel.

Calvert lists three possible approaches to developing practical hydrogel-based actuators:

- "Develop a chemical actuator with a compact and reliable supply of the needed chemical energy, not necessarily depending on acid and base.
- Develop a thermal actuator based on expansion against a piston of a gel within a porous but rigid enclosure, similar to an automobile radiator thermostat.
- Develop a two-compartment fine scale electrically driven gel muscle as an extension of the electrically-driven PAN fibers." [2]

Besides artificial muscles, gels have been the subject of additional academic research, including the actuation of valves and pumps, for drug delivery in adhesive patches or implanted devices with electrically-controlled release mechanisms, and for sensors of pH and other liquid properties. Currently, useful gel actuators are elusive, but recent developments have made significant progress toward their practical usefulness [2].

K. Research in Hydrogel Actuators

Bassil et al. have described the actuation mechanism of polyacrylamide hydrogels. Under electrical stimulus, the bending behavior is caused by a pH gradient due to ions produced inside the polymer matrix. At the cathode, hydrogen is expelled and hydroxide ions are formed, and this region becomes more basic. Similarly, at the anode, oxygen is expelled, hydronium ions are formed, and this region becomes more acidic. This pH difference creates a difference in strain through the thickness of the material. Shrinking induced by an external change in pH is cause by the expulsion of ions from the gel matrix. They also measure volume changes and the time taken to reach a bending angle of 90° with an applied voltage (Figure 9). Gels with a thickness of 2 mm exhibited bending speeds of 60°/s, which is faster than traditional polypyrrole actuators in air [43]. Others have explored the swelling behavior of polyacrylamide [44] and poly(vinyl alcohol)/poly(acrylic acid) composites [45]. Kim et al. studied the electroactive characteristics of a poly(vinyl alcohol)/poly(*N*-isopropylacrylamide) composite, and found that an electrically-activated actuator could be created. They found that a 30-mm thick sample exhibited a bending angle of 50° after 60 s under an applied voltage of 20 V in conditions similar to the human body, and that a repeatable bending/relaxation cycle was possible by the toggling of an applied DC voltage [46]. Shang et al. investigated the electroactive properties of a hydrogel based on a natural material, chitosan. The chitosan composite demonstrated a bending angle of 80° after 20 s in solution with an applied voltage of 15 V. The authors also characterize the mechanical properties of the composite (Young's modulus, breaking strength, % elongation) as a function of cross-link density

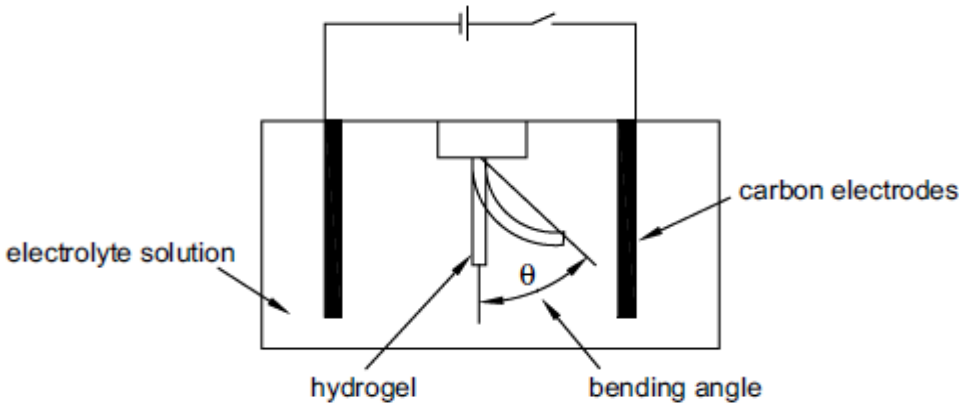

Figure 9. Apparatus for measuring the bending angle of a hydrogel in an applied electric field. From [47].

[47]. Shim and Lee synthesized electroactive and temperature-sensitive composites of poly(*N*-isopropylacrylamide) and polypyrrole, another electroactive polymer [48]. Research into hydrogel composites as hydrogel actuators shows promise, but new materials and methods need to be devised in order to replicate the properties of natural muscle.

L. Poly(NIPAAm)

Poly(*N*-isopropylacrylamide) [poly(NIPAAm)] is a thermosensitive hydrogel with a LCST of about 32°C, and for this reason, has attracted much attention from research in the medical and pharmaceutical fields (Figure 10). Pure poly(NIPAAm) is soluble in water below its LCST and appears transparent, but becomes hydrophobic and precipitates out of aqueous solution above its LCST, because it exists in a coiled state at low temperatures and a globular state at higher temperatures. Since this phase transition is near the temperature of the human body, poly(NIPAAm) has been suggested for drug

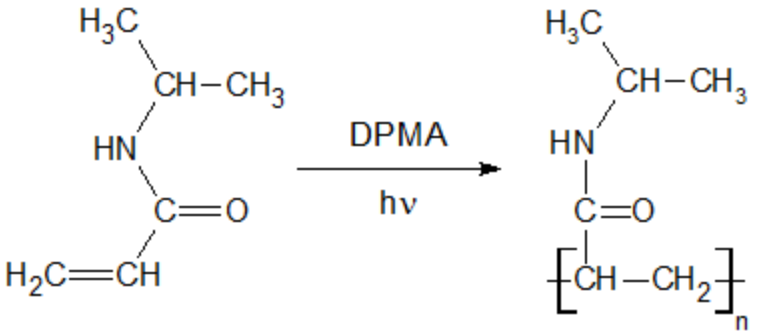

Figure 10. The UV-initiated free radical polymerization of *N*-isopropylacrylamide to form Poly(*N*-isopropylacrylamide) [poly(NIPAAm)].

delivery or soft tissue replacement. By synthesizing cross-linked poly(*N*-isopropylacrylamide-*co*-acrylic acid) with varying concentrations of acrylic acid the LCST could be adjusted. Specifically, the more hydrophilic monomers exist in the polymer backbone, the higher the LCST is, because of the increased solubility of the polymer chain [49]. Many techniques have been described for the creation of macroporous poly(NIPAAm) [42]. Because of its many useful properties, poly(NIPAAm) was chosen to form the base of the novel composite described in this work.

II. REVIEW OF LITERATURE TECHNIQUES

A. Gold Nanoparticle Synthesis

13-nm gold nanospheres were prepared from solutions of $HAuCl_4$ (Sigma-Aldrich) and sodium citrate (Fisher) by a standard procedure for later usage. 20 mL of 1.0 mM $HAuCl_4$ was heated while stirring until the solution boiled. Then 2 mL of 38.8 mM sodium citrate solution was added, which causes the solution to darken over the course of several minutes. This solution of citrate-capped gold nanospheres appears deep red in color [50].

The previously prepared 13-nm gold nanospheres, as well as 4-nm gold nanospheres prepared by the reduction of $HAuCl_4$ by sodium borohydride (Fisher) at 0°C, were used to prepare gold nanorods. Briefly, 20 mL of seed solution is made by the mixing of 18.4 mL deionized water (Millipore Milli-Q Gradient), 0.5 mL of a 0.01 M $HAuCl_4$ solution and 0.5 mL of 0.01 M sodium citrate. An ice-cold solution of 0.1 M sodium borohydride is quickly added to this solution while stirring. When prepared, Murphy's group reports that this procedure yields a pink solution containing citrate-capped gold nanospheres. These results were not reproducible; a similar solution of nanospheres appeared deep purple. Murphy and coworkers developed a three-step procedure in which a solution of gold nanospheres is transferred into successive vials of a growth solution containing a surfactant-Au(I) complex. The aspect ratio of the nanorods is affected by the length of the carbon chain on the surfactant [51]. In this synthesis, cetyltrimethylammonium bromide (C_{16}TAB) obtained from MP Biomedicals was used as

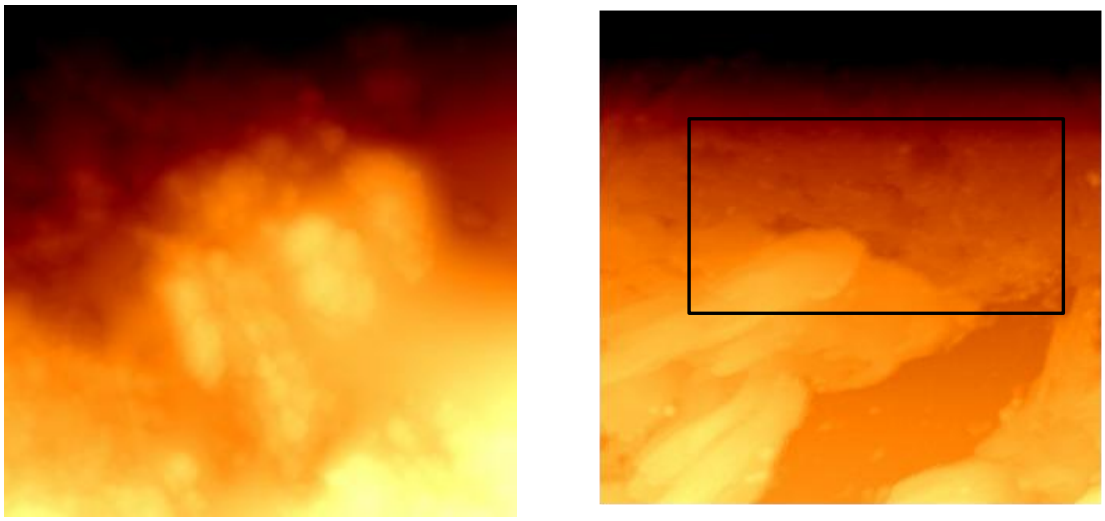

(a) (b)

Figure 11. AFM imagery (300 nm x 300 nm) of gold nanoparticle solution subjected to the nanorod synthesis method suggested by Murphy [51, 52]. (a) Significant gold nanoparticle accumulation has occurred. (b) Aligned nanorods can be seen at the top of the image.

the surfactant. As the synthesis proceeds, the purple solution of nanospheres turns pinkish-purple through dilution and further nanorod growth. Murphy's group reported nanorods with an average aspect ratio of 23 ± 4 using C_{16}TAB to direct nanorod growth. They theorize that surfactants preferentially adsorb to specific faces of the gold, thus stopping further nanoparticle growth in those directions. Furthermore, a surfactant bilayer forms adjacent to the inhibited faces, thus directing the expansion of the nanoparticle into an elongated shape [52].

Unfortunately, atomic force microscopy (AFM) imaging revealed significant nanoparticle agglomeration, which made preparation of gold nanorods difficult (Figure 11). The synthesis of gold nanorods appeared to be unrepeatable, with identical solutions producing different results, as evidenced by the solution color of the three-step process after completion. This difference may be due to differing nanoparticle sizes in the seed solution. When a solution containing 13-nm gold nanospheres was subjected to this

procedure, little or no result was observed, perhaps because the nanospheres must be below some critical diameter for the surfactants to align to direct secondary growth.

B. Hydrogel Synthesis

Cross-linked poly(NIPAAm) samples were prepared according to a modified version of Hilt's method. *N*-Isopropylacrylamide (NIPAAm) was used as the monomer, poly(ethylene glycol) 550 dimethacrylate (PEG550DMA) was used as a cross-linker, and 2,2-dimethoxy-2-phenylacetophenone (DMPA) was used as a photo-initiator. All materials were obtained from Sigma-Aldrich. NIPAAm and PEG550DMA were mixed in 90:10, 80:20, 70:30, 60:40, and 50:50 molar ratios and dissolved in an equal weight of ethanol (Fisher) (Table 1). DMPA was added in the amount of 1% of the total weight of NIPAAm and PEG550DMA together, and the mixture was vortexed in a light-proof vial until the DMPA was dissolved. The mixture was pipetted in 1 mL portions to two glass plates separated by a 1 mm PDMS (Sylgard 184, Dow-Corning) spacer and held together by clamps, and placed under an ultraviolet light (American UV Co. Model PC-100S) to polymerize for 5-10 minutes. After polymerization, the hydrogel samples were removed from the molds and stored in deionized water to prevent drying and cracking [36, 53]. These samples were used as the base of the hydrogel-polyaniline composite described later.

Table 1. The composition of hydrogels with various monomer:crosslinker ratios.

	90:10	80:20	70:30	60:40	50:50
NIPAAm (mg)	791.1	627.4	495.0	386.7	295.7
PEG550DMA (μL)	104.7	186.7	252.6	306.9	352.2
Ethanol (mL)	0.896	0.814	0.748	0.693	0.648
DPMA (mg)	8.96	8.14	7.48	6.93	6.48

C. Polyaniline Synthesis Techniques

Different synthesis and processing techniques can be used to create different polyaniline nanostructures [17]. It is known from early experiments with electropolymerization that polyaniline can form in fibers of approximately 100 nm on the surface of the electrodes. Based on this knowledge and observations that small nanofibers formed early on in the polymerization reaction, it was hypothesized that secondary growth of polyaniline could be suppressed to yield almost pure nanofibers as a product. There are two methods of achieving this goal: Diffusion across a liquid-liquid interface (intrafacial polymerization) and limiting initiator access to the nascent nanofiber, which is accomplished via rapidly mixed reactions [18]. However, neither of these methods provides directionally- conductive polyaniline without a further processing step such as spinning or drawing fibers, as is described in this work.

Huang et al. developed a procedure to manufacture polyaniline nanofibers of relatively uniform diameter (averaging 50 nm) based on diffusion between organic and aqueous phases [54]. They demonstrated that these nanofibers could be used as sensors for the presence of HCl vapor. Since HCl dopes polyaniline and increases its conductivity, the resistance of the system decreases as a function of time [20].

Huang et al. reported a simple method to polyaniline nanofibers with a relatively tight distribution of diameters (30 – 50 nm) with lengths ranging from 500 nm to several microns by the diffusion of aniline from an organic phase into a less-dense aqueous phase containing an initiator and a doping acid. Polymerization occurs across the aqueous-organic interface, and the doped polyaniline diffuses into the aqueous phase, which turns homogenously dark green after 24 hours. The polyaniline can be separated by dialysis [20, 54] or simple filtration.

Wang et al. prepared polyaniline nanostructures in a similar fashion, placing the aqueous phase in the reaction vessel first and using a thin layer of liquid paraffin to separate the aqueous and organic phases. Diffusion of aniline through the paraffin layer and into the aqueous layer, again containing an initiator and a dopant, yielded microstructured polyaniline. Depending on the reaction conditions, nanofibers, nanosheets, or nanoclusters could be formed (Figure 12) [55]. 0.80 mmol of ammonium persulfate (APS, Acros Organics) was dissolved in 10 ml of 2.0 M HCl solution (Fisher) and poured into the bottom of a test tube. Approximately 1 mL of liquid paraffin (Acros, boiling point > 300°C) was carefully layered onto the aqueous layer. 3.2 mmol of aniline (Acros, used as received) was dissolved in a mixture containing 3.3 mL of hexanes (95% n-hexane, Acros) and 6.7 mL of mixed xylenes (Fisher). This mixture was carefully poured into the test tube in such a way as to avoid disturbing the paraffin layer, thus keeping the layers separate. Almost immediately, dark green threads of HCl-doped polyaniline began to form in the aqueous layer. The reaction was allowed to proceed overnight. The next day, the aqueous layer was uniformly dark green and the aqueous layer was reddish-brown due to the presence of aniline oligomers [55]. The organic layer

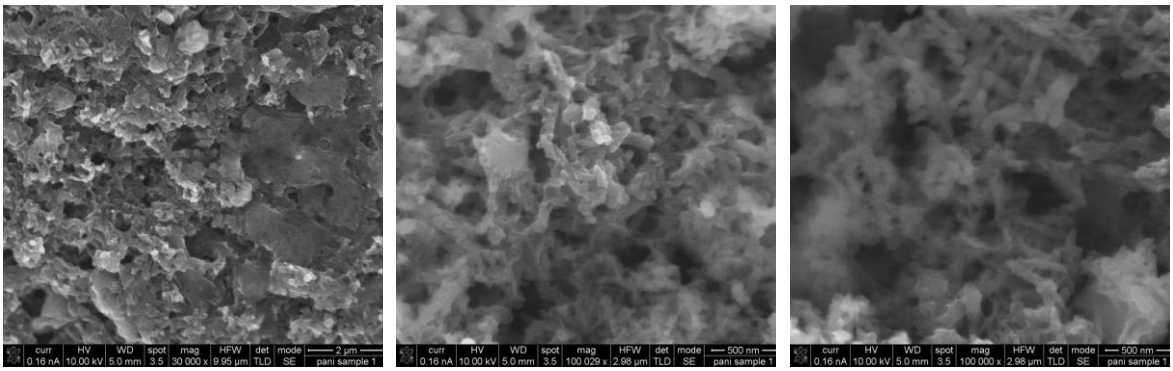

(a) (b) (c)

Figure 12. Polyaniline prepared by our group by the method of Wang et al. (ref. [55]) viewed by scanning electron microscopy (SEM). (a) 30,000x magnification. (b) and (c) 100,000x magnification. Nanofibers approximately 400 nm in length and 90 nm in diameter can clearly be seen at higher magnifications.

and paraffin were carefully pipetted off and the aqueous layer was filtered and left to dry in the open air, then stored in a dehumidifier.

It is known that polyaniline created in rapidly-mixed reactions tends to have a nano-fibrillar structure. Li et al. developed a template-free synthesis method to create polyaniline "nanosticks" with average diameter 40 nm and lengths of 300 nm or longer. These nanosticks form stable suspensions in water in the absence of stabilizers such as surfactants, unusually for polyaniline. They report peak conductivities of 2.23 S/cm when polymerized in 2.0 M HNO_3 and that the nanosticks can be used to form semiconductive nanocomposites with insulating polymers such as poly(vinyl alcohol) [56].

Nanosticks were synthesized using a modified version of this method, with HCl as the dopant acid instead of HNO_3. 80 mL of a 2.0 M HCl solution and 0.91 mL of aniline were placed in a 250-mL beaker and stirred vigorously with a magnetic stirrer. A solution containing 2.28 g of APS in 20 mL of 2.0 M HCl was placed in a syringe pump (Cole-Parmer 74900, 60 mL syringe) and set to add the solution over the course of 30 min. The solution was continually stirred over 6 hr. At the end of 6 hr, the solution

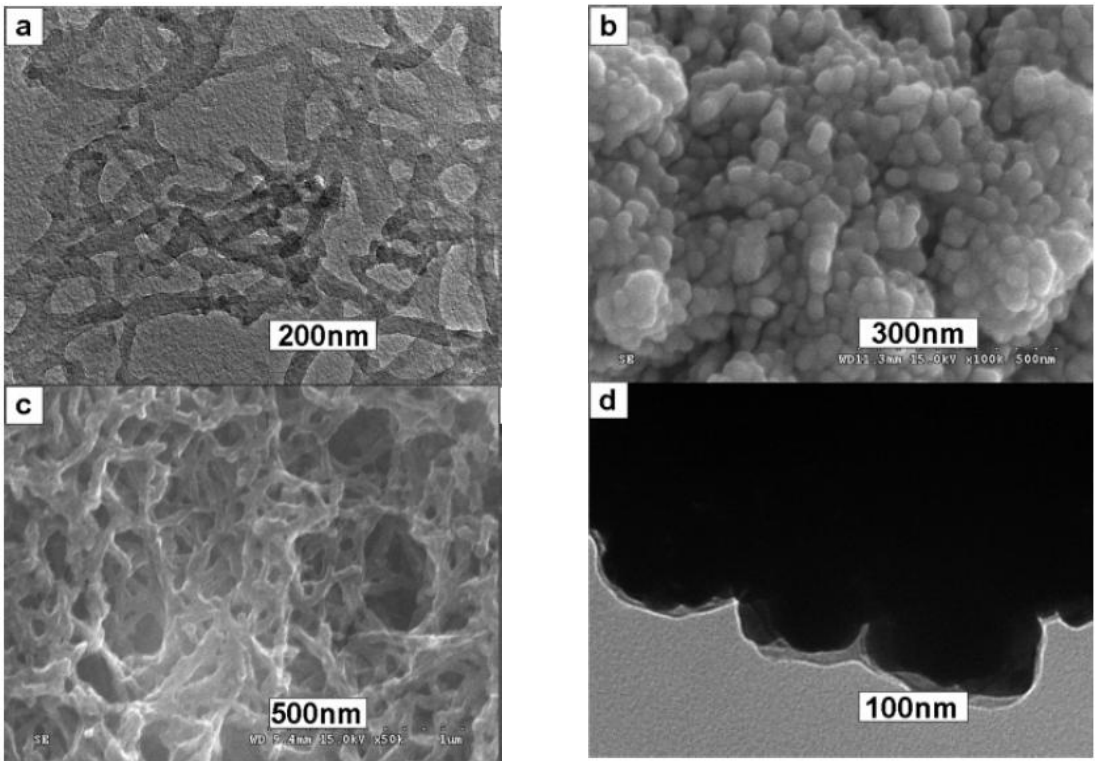

Figure 13. (a) TEM image of polyaniline nanofibers prepared by Wang et al. (b) SEM image of agglomerated gold nanoparticles. (c) SEM image of a thin film of nanofibers. (d) TEM image of gold particles, showing that they are coated in a thin layer of polyaniline. From [57].

appears greenish-black with a thin, oily-looking film presumably containing polyaniline nanosticks floating on the surface. The nanosticks were separated from the bulk suspension by centrifugation (Eppendorf 5702, 3500 rpm) and washed with deionized water, then air-dried and stored in a dehumidifier. The nanosticks were pressed between steel disks approximately 1 cm in diameter for resistivity measurements. The resistance of these samples was measured simply by two multimeter leads placed approximately 1 mm apart, giving a value of R = 7 kΩ. This gives a conductivity measurement of 1.4 × 10^{-4} S/cm.

Wang et al. reported the synthesis of polyaniline nanofibers using $HAuCl_4$ as the oxidant. Briefly, 5 mmol of aniline was dissolved in 20 mL of 1 M HCl solution and

mixed vigorously with a 0.05 M $HAuCl_4$ solution. The solution gradually changes colors from light yellow originally to darkening shades of blue and finally dark green, indicating the presence of doped polyaniline. When polyaniline is formed the reduction of $HAuCl_4$ in the absence of HCl as a doping agent, a dark reddish solution is obtained instead. The solution was allowed to mix for 24 hours, after which the stirring was stopped and gold particles slowly precipitated out of solution. The polyaniline nanofibers were collected by centrifugation, washed with deionized water, and left to dry. The authors report the conductivity of the nanofibers to be 0.16 S/cm as measured in a pressed-pellet format by the four-point probe method, which is typical of HCl-doped polyaniline.

SEM and TEM images reveal the dark green product to be a tangled network of polyaniline nanofibers approximately 35 nm in diameter (Figure 13). Interestingly, the gold particles appear to be agglomerations of many gold nanoparticles, all coated in a thin layer of polyaniline, and appear to be of similar diameter to the polyaniline nanofibers. The authors propose that initial nanoparticle formation may catalyze the polymerization of aniline due to the adsorption of aniline monomers and oligomers onto certain crystal faces, due to the similarity of diameters between the polyaniline nanofibers and the gold nanoparticles and the thin layer of polymer on the surface of the agglomerated nanoparticles [57].

D. Composites

Mallick's group synthesized a gold nanoparticle-polyaniline composite material by the one-step polymerization of aniline by the reduction of $HAuCl_4$. Unusually for

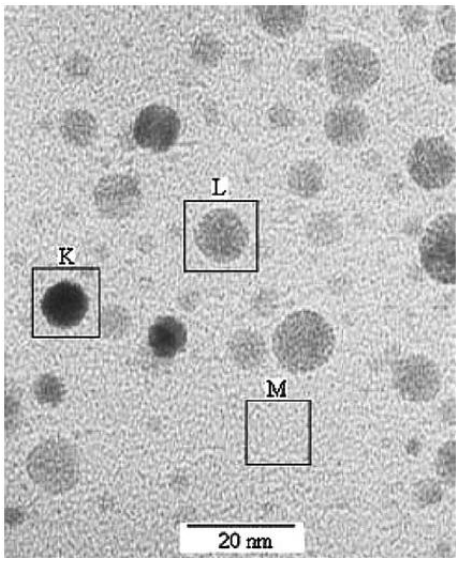

Figure 14. TEM image of the gold-polyaniline nanocomposite prepared by Mallick et al. (K) A gold nanoparticle on the surface of the composite (L) A gold nanoparticle inside the bulk polyaniline. (M) An area with no nanoparticles. From [32].

nanocomposites, the gold nanoparticles produced are comparatively small, 6 – 7 nm as confirmed by transmission electron microscopy (TEM) (Figure 14). The bulk of the nanoparticles formed are encapsulated inside the polymer phase. They hypothesize that the reaction proceeds by the protonation of aniline followed by the reduction of the $[AuCl_4]^-$ ion. During polyaniline formation, electrons are released, which reduce the gold ions to neutral gold atoms, which agglomerate into nanoparticles, which are stabilized and protected from further growth by the surrounding polymer matrix. To prepare the composite, a modified version of this procedure was used [32]. 0.08 g of aniline was dissolved in 5 mL of ethanol. To this solution, 3.5 mL of a 0.01 M $HAuCl_4$ solution was added dropwise, which caused a gradual color change of the solution from colorless to red and become filled with a suspended solid. The solution was cast onto a plate and allowed to air-dry, after which a thin layer of a reddish-brown material was observed on the bottom of the plate. The solid was scraped from the plate and stored in a dehumidifier

until use. A similar version of this procedure was reported by Kinyanjui and Hatch using HBF_4 as the doping acid [58].

Initial attempts at using the nanosticks to increase the conductivity of insulating polymers were fraught with difficulties. Various concentrations of the nanosticks, as well as 4-nm gold nanoparticles, were added to solutions of acrylamide (AM, Sigma-Aldrich) in deionized water, using DPMA as an initiator, and polymerized under UV radiation. At high concentrations (above 5% by weight of the additive compared to the monomer), polymerization was poor, probably due to the opacity of the solution, and very little solids were observed in the vessels used for UV polymerization.

Subsequently, smaller concentrations of the nanosticks, as well as samples of the gold-polyaniline nanocomposite, were used to prepare samples in a similar fashion (Table 2). The molds used to hold the samples for UV polymerization were filled with sticky solids, which had polymerized much better than previous attempts, even though the solutions were still dark in color. The resistance of these samples was measured by a simple two-point probe method with the approximately 1 mm apart. However, distribution of the additives in the bulk polyacrylamide (PAM) was poor. Particles are still visible even at low magnifications. Lower concentrations of the additives would have been difficult to measure due to their very small weights.

Table 2. The composition of polyacrylamide composites with various conductivity-enhancing additives, as measured by our group.

	0.75% Nanosticks	1.5% Nanosticks	1% Nanocomposite
Acrylamide (mg)	203.9	203.8	203.7
DPMA (mg)	23.0	22.7	23.0
Additive (mg)	1.5	3.0	1.8
DI water (μL)	400	400	400
Resistance (MΩ)	1.3	2 – 3	6
Conductivity S/cm	7.7×10^{-8}	$3.3 – 5 \times 10^{-8}$	1.6×10^{-8}

Xiang and Xie prepared a unique copolymer consisting of polyaniline grafted onto a polyacrylamide backbone which is soluble in alkaline solutions. They reported that thin films could be cast from solutions of the polymer in sodium hydroxide and subsequently doped with either HCl solution or gas to increase conductivity. The authors explored several molar ratios of monomers, observing that conductivity increased as the molar ratio of aniline to acrylamide increased (up to 8.8 S/cm at a molar ratio of 15). They also found that no graft copolymerization occurred when aniline was polymerized under similar conditions in the presence of poly(acrylic acid) or poly(vinyl alcohol), and hypothesize that the grafting site of the polyaniline branches is the nitrogen atom of polyacrylamide [59]. Polymer composites consisting of polyaniline and poly(acrylic acid) [60] and polyaniline and poly(vinyl alcohol) [61] have been prepared; presumably these composites are merely bulk mixtures and contain no actual chemical cross-links between the polymers.

This process was carried out by a modified version of the original. The polymerization of acrylamide was effected by the addition of 1 g of acrylamide to 10 mL of deionized water, followed by the addition of 1.5 mg of APS as an initiator. The entire mixture was degassed by bubbling nitrogen gas through it for 30 minutes and sealed, then placed in a boiling water bath for 2 – 3 hours. At the end of the polymerization, a viscous solution of light yellow polyacrylamide in water is obtained. The authors measured the number average molecular weight to be $\overline{M}_n$ = 4.8 – 5.5 × 10^5 g/mol. Oxidative polymerization of other monomers, such as acrylic acid (Acros), methacrylic acid, methacrylamide (Sigma-Aldrich), and NIPAAm was conducted in the same way. All yielded clear to light yellow viscous solutions of their respective polymers.

The solution obtained previously is used directly in the graft copolymerization with aniline. The solution is mixed with an equal volume of 2 M HCl to make the final concentration of the solution 1 M. Aniline (distilled before usage and refrigerated) was added to the solution in such an amount as to obtain a 15:1 molar ratio of aniline to acrylamide. 1 mol of APS dissolved in a 1M solution of HCl was added dropwise from a buret into the solution over the course of several minutes with vigorous stirring while placed in an ice bath, and the copolymerization reaction was allowed to proceed for 3 hr. After the reaction was completed, the darkly-colored solution was filtered, and the residue was washed with deionized water and dissolved in 1 M NaOH (Fisher). This suspension was filtered again, and then the residue was dried to obtain dark green homo-polyaniline and polyacrylamide-*graft*-polyaniline (PAM-*g*-PAni) with high aniline to acrylamide ratio. The authors state that the filtrate of this solution could be dialyzed to remove the residual salts and then dried to obtain the alkali-soluble and conductive PAM-*g*-PAni with a low aniline to acrylamide ratio [59]; however, this approach was not tried due to the lack of materials.

The same procedure was also attempted using other, novel monomers as the backbone for grafting. Graft polymerization in the presence of poly(acrylic acid) and poly(methacrylic acid) gave no reaction, but polymerization in the presence of polymethacrylamide and poly(NIPAAm) appeared to give similar results as polymerization with PAM. The initial filtration of the completed reaction yields an orange filtrate from acrylamide, which gives a dark green residue which forms chunks when dried. Similarly, the initial filtration of the completed poly(NIPAAm) grafting reaction yielded a reddish-brown filtrate and a purplish-green solid which forms small

plates when dried. Upon dissolving the residues in 1 M NaOH, a dark blue solution was obtained, from which was filtered *graft*-PAni with a high aniline to monomer ratio. These residues were washed with deionized water and left to dry, after which they were pressed into disks between steel plates for analysis. The residue containing PAM-*g*-PAni appeared dark bluish-purple with a bronze glint on the surface, while the residue containing poly(NIPAAm)-*g*-PAni appeared dark brown with a bronze glint and also contained patches of dark purple. These descriptions closely match the description of dedoped PAM-*g*-PAni as given by the authors. Due to dedoping by exposure to NaOH, these polymer samples are non-conductive; however, their conductivity could be restored by soaking in 1 M HCl and redrying. Doing so yielded doped PAM-*g*-PAni, which appeared to be made of large green and purple particles, and poly(NIPAAm)-*g*-PAni, which appeared to be mostly made of small green particles, perhaps due to a lower poly(NIPAAm) content. If the grafting site is the nitrogen atom of the acrylamide monomer, the bulky *N*-isopropyl group of NIPAAm would tend to shield the atom from attack.

After this second filtration, a blue filtrate remained from the PAM grafting reaction, and a light tan filtrate remained from the poly(NIPAAm) grafting reaction. The authors stated that these filtrates contained *graft*-PAn with a low aniline to monomer ratio. This solution also contains a good deal of dissolved salts, which make casting thin films of this polymer impossible [59]. It was attempted to extract the *graft*-Pan into an organic solvent so that a thin film could be deposited, but evidently the *graft*-Pan is insufficiently soluble in the solvents tried (hexanes, xylenes) that no polymer was

transferred from the aqueous to the organic phase. Thus, the results of this synthesis were intractable and could not be characterized.

Athawale and coworkers synthesized polyaniline doped with acrylic acid, and noted a higher conductivity and greater solubility in organic solvents than polyaniline doped with HCl. HCl- doped polyaniline was synthesized by a simple method described in the literature. 2.3 g of APS were dissolved in 25 mL of 1.5 M HCl. This solution was placed in a syringe pump and added over the course of 3 hr to a vigorously stirred solution containing 2 mL of aniline (distilled before usage and refrigerated) dissolved in 25 mL of 1.5 M HCl placed in an ice bath. After the oxidant solution was completely added, the reaction was allowed to continue for an additional hour. The suspension was filtered, then the polyaniline residue was washed with deionized water and ethanol until the rinse was cleared. It was then rinsed twice with diethyl ether (Fisher) and dried [62, 63].

To produce acrylic-acid doped polyaniline, 0.2 mL of acrylic acid was added to the aniline solution prior to the addition of the initiator, and the mixture was stirred for 24 hr. The authors dissolved the acrylic acid doped polyaniline in *m*-cresol and *N*-methyl pyrrolidinone (NMP), and noted an approximate doubling of the solubility of polyaniline in each solvent. They attributed this to the presence of a greater number of charges on the polyaniline chain, which leads to increased hydrogen bonding between the polymer and the solvent, and hypothesize that this causes the polymer chain to adopt an expanded coil or linear structure in solution rather than a compacted coil. The larger number of charges would also cause intramolecular repulsions between sections of the polymer chain. UV-visible (UV-vis) spectroscopy and Fourier transform infrared spectroscopy (FTIR) were

used to describe the spectra of the solutions, and identified that acrylic acid acts as a pseudo-protonic acid by coordinating with the imine nitrogen atom in the emeraldine form of polyaniline, thus decreasing the tendency of the chain to hydrogen bond with itself. This leads to disaggregation of the coiled structure and greater crystallinity and conductivity. HCl, on the other hand, is a protonic acid, which causes increased hydrogen bonding, and subsequently aggregation, of the polyaniline chain, which reduces conductivity. The authors measured the conductivity of acrylic acid doped polyaniline to be 6.20×10^{-3} S/cm, as compared to 2.09×10^{-3} S/cm for HCl doped polyaniline [63].

This acrylic acid doped polyaniline was also reasonably soluble in its parent acrylic acid, which sparked an interesting idea: Could a conductive hydrogel be formed by the polymerization of acrylic acid containing polyaniline? To test this hypothesis, a small amount of acrylic acid doped polyaniline was added to pure acrylic acid and thoroughly mixed. The suspension was allowed to stand and then filtered, leaving a light yellow-green solution of polyaniline in acrylic acid. This mixture was used as the monomer to prepare a gel with 90:10 monomer to crosslinker ratio, in the same manner as recommended by Hilt's group. This solution was then subjected to UV polymerization as before [36]. After removal from the mold and soaking in deionized water to remove any residual monomer or salts, the resistance of these samples was measured to be approximately 600 kΩ by a simple two-point probe method with the approximately 1 cm apart. This translates to a conductivity of approximately 1.67×10^{-6} S/cm, as compared to a conductivity of approximately 10×10^{-11} S/cm for unmodified poly(acrylic acid) at room temperature [64]. This represents an outstanding 10^5-fold increase in conductivity,

and is an area which could be investigated further. A similar concept, the increase of the solubility of polyaniline by complexing it with a polyelectrolyte, has been reported [65].

E. Surface Polymerization of Polyaniline

Das et al. described a method of synthesizing a polyacrylamide-polyaniline composite with moderate conductivity by exposing a film to polyacrylamide to aniline vapor. They cast films containing polyacrylamide ($\overline{M}_w = 5 \times 10^4$ g/mol) and APS from aqueous solution, then exposed the films sequentially to HCl and aniline vapors. Doped polyaniline formed on the surface of the polyacrylamide films with increasing opacity as the time of exposure increased. The authors found that as the amount of time the samples

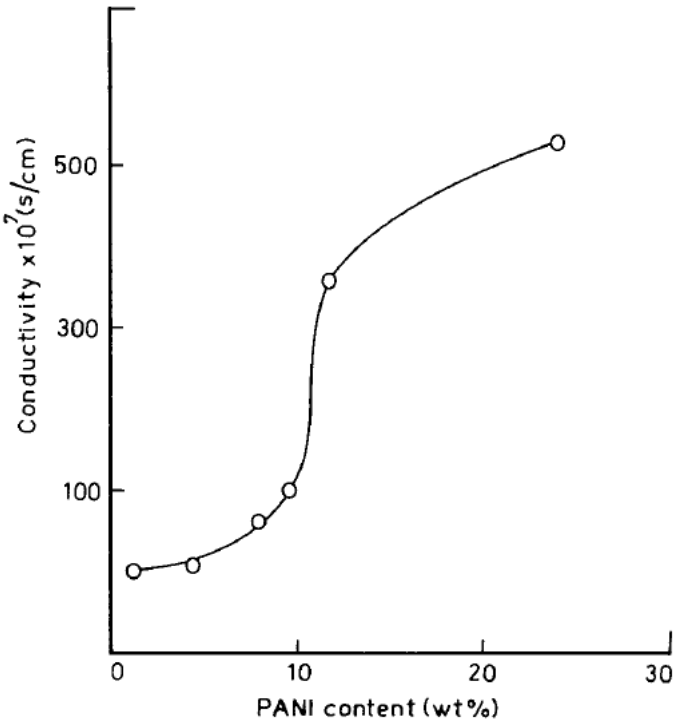

Figure 15. Plot of conductivity of a polyacrylamide-polyaniline composite as a function of weight percent polyaniline. From [66].

were exposed to the aniline vapor increased, the weight percentage of polyaniline in the samples increased, and so did the conductivity. The plot of conductivity of the composite as a function of weight percent polyaniline is strongly non-linear with a sharp increase in conductivity at approximately 11.5%, with a much slower increase in conductivity after that value is reached (Figure 15) [66].

F. Conclusions

The current literature provides a myriad of synthesis and processing techniques for polyaniline and polyaniline composites, just a few of which are detailed here. However, none of these synthesis techniques yielded a conductive hydrogel with properties that we felt furthered the objectives in constructing a composite which exhibited the properties necessary to create artificial muscle for left ventricular assist devices. Therefore, new methods of synthesis were attempted, which lead to the creation of the novel polyaniline hydrogel composite described *vide infra*.

III. A NOVEL SYNTHESIS TECHNIQUE: PATTERNING OF POLYANILINE BY SURFACE POLYMERIZATION

A. Introduction

In this thesis, we report the synthesis of a novel polyaniline-hydrogel composite with several unique properties, at least two of which has not yet been reported in the literature as far as we are aware. First, this composite exhibits directional conductivity in unaligned polyaniline chains. As far as we are aware, directional conductivity has previously been produced in polyaniline by a post-synthesis step such as physically drawing or spin-coating polyaniline from solution [67], or by a chemical modification of the base polyaniline structure [68]. Second, it involves the directed synthesis of a polymer by surface polymerization of a monomer in the vapor phase using PDMS templates. To our knowledge, only nanoparticles have been synthesized by vapor deposition directed by PDMS templates [69]. Third, it is a simple, low-cost, customizable, and efficient method for producing a composite with exciting properties, without the difficulties associated with processing polyaniline after it is synthesized. The materials involved are easily acquired from chemical suppliers, relatively non-toxic and easily handled compared to other materials used in the literature. For artificial muscles to become an economically viable alternative to current medical solutions such as prosthetic limbs, the processes involved for creating the materials involved must have these properties.

In this research, simple patterns of lines were chosen for ease of template fabrication as well as general applicability to fields as diverse as biomedical applications and flexible circuit boards. Conceivably, these template patterns could be made as complex as necessary or reduced in size using micro- or nano-scale template fabrication. It is hoped that by providing a preferred direction of transport for electrons, a corresponding gradient in ion concentration will cause bending in a specific direction. Two methods of depositing patterned polyaniline were investigated: vapor and liquid.

B. Vapor Deposition

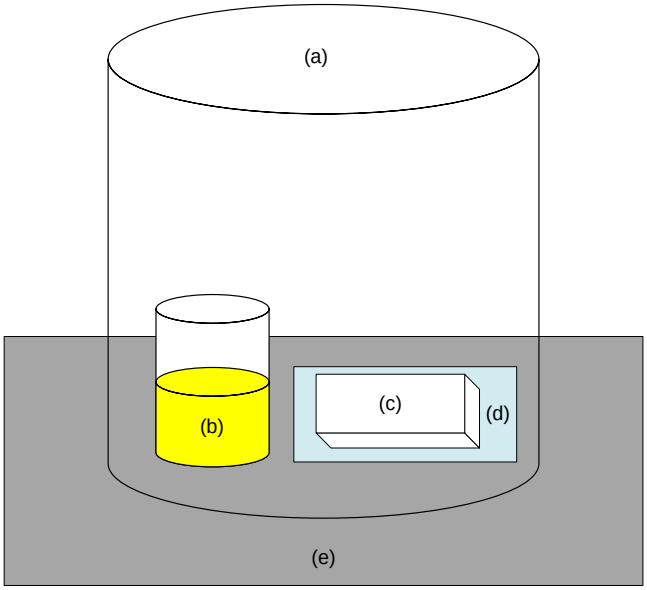

Figure 16. Schematic of setup for surface polymerization of polyaniline by vapor deposition. (a) 250-mL beaker. (b) Glass vial containing a few mL of liquid aniline. (c) Poly(NIPAAm) sample. (d) Glass microscope slide. (e) Aluminum foil (2 layers).

Thin films of cross-linked poly(NIPAAm) with molar compositions prepared as was discussed earlier were soaked overnight in a solution containing 1M HCl and 0.1 M APS. In the first method, the films were placed on a glass microscope slide, which was placed on a piece of aluminum foil with a small vial containing a few milliliters of liquid

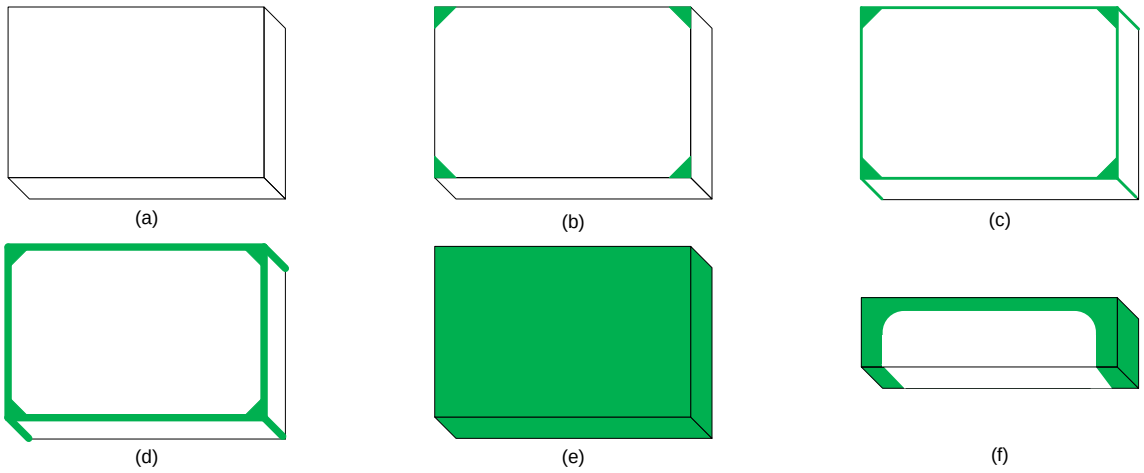

Figure 17. Progression of the surface polymerization of polyaniline onto a poly(NIPAAm) sample by vapor deposition (dimensions have been exaggerated for clarity). (a) No exposure to aniline vapor. (b) After 2 min. (c) After 5 min. (d) After 10 min. (e) After 24 hr. (f) Cross-section of the material after 24 hr.

aniline. A 250-mL beaker was placed over the entire setup, the edges of the foil were folded up to form a seal, and the setup was allowed to stand at room temperature. Within several minutes, green polyaniline began to form on the edges of the poly(NIPAAm) sheet, indicating that aniline in the vapor phase was reacting with the HCl and APS in the poly(NIPAAm) sample. If the poly(NIPAAm) sample is unobstructed, a thin layer of polyaniline will form on any exposed surface. This occurs over the course of several hours at room temperature, with all five exposed faces becoming coated in a thin layer of solid conductive polyaniline. The samples were then soaked in deionized water overnight to remove any residual salts. Cross-sections taken from samples indicate that the polyaniline penetrates 0.1 – 0.2 mm into the bulk poly(NIPAAm). The resistance of samples prepared in this way as measured by electrodes 7 mm apart was approximately R = 100 kΩ, which gives a conductivity of 1.43×10^{-5} S/cm.

However, the deposition of polyaniline onto the poly(NIPAAm) sample can be directed by the use of PDMS stamps to selectively block portions of the sample from

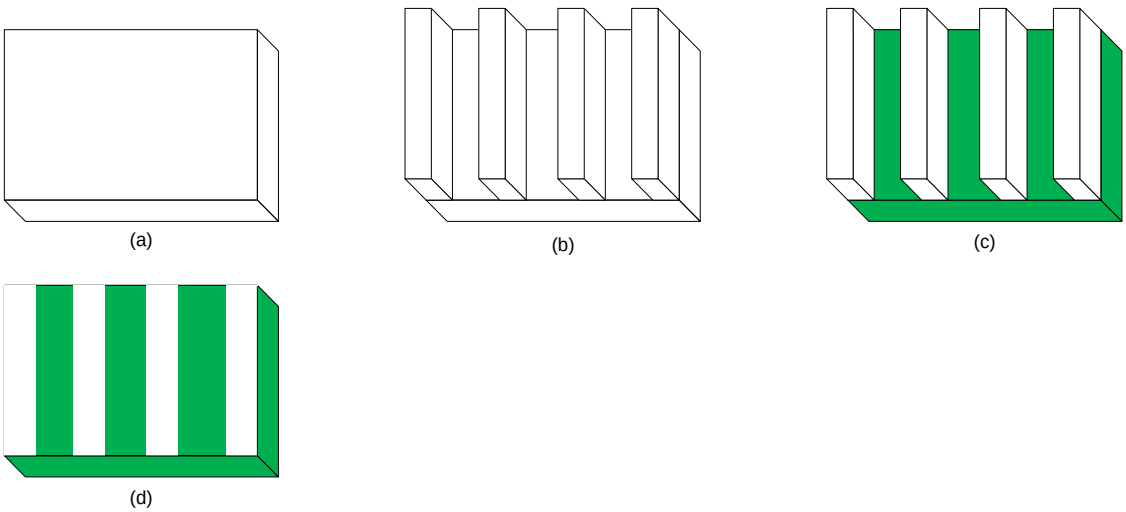

Figure 18. Progression of the surface polymerization of polyaniline onto a poly(NIPAAm) sample by template-assisted vapor deposition (dimensions have been exaggerated for clarity). (a) No exposure to aniline vapor. (b) PDMS stamp is applied to surface. (c) After exposure to aniline vapor. (d) PDMS stamp is removed, showing patterned polyaniline-hydrogel composite.

direct exposure to aniline vapor. In this way, patterns of polyaniline can be created. In a typical synthesis, a poly(NIPAAm) film approximately 1 cm × 1 cm × 1 mm was left to soak in a solution containing 1 M HCl and 0.1 M APS for 24 hr. This sample was surface-dried, then a "stamp" consisting of strips of PDMS approximately 1 cm × 1 mm × 0.2 mm was placed on the surface such that the strips were approximately 1 mm apart and aligned in a parallel fashion. This setup was then placed in the reaction chamber described earlier for 24 hr. After reaction, the sample was removed from the chamber and the PDMS strips removed from the sample, revealing that no polymerization had occurred in the areas occluded by the "stamp". In this way, composites containing patterned areas of polyaniline could be produced in a simple and inexpensive manner. Images of the patterned samples prepared by vapor deposition are shown in Figures 19 and 20.

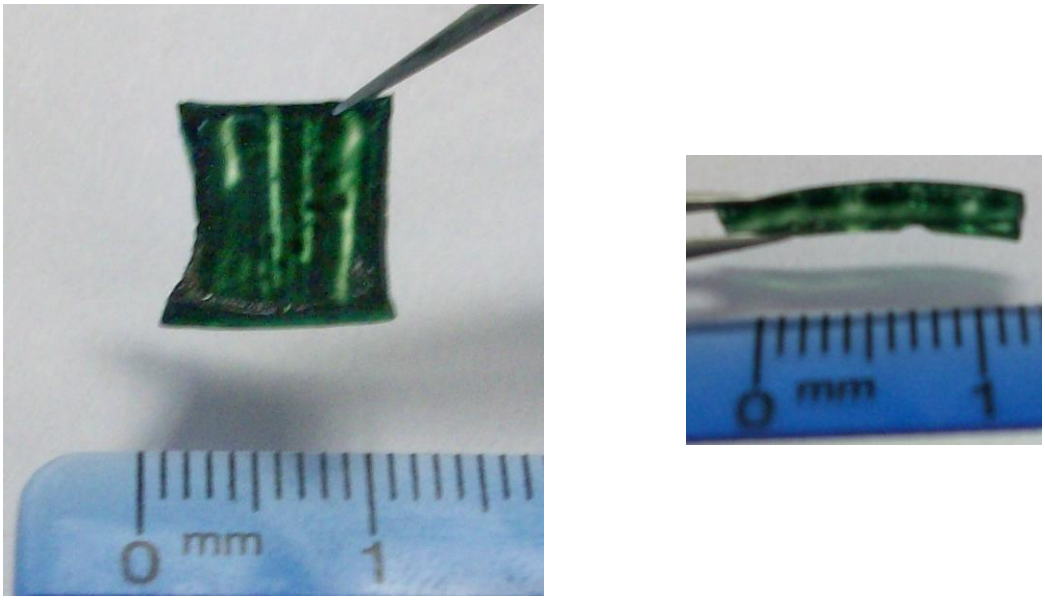

(a) (b)

Figure 19. Photographs of the patterned polyaniline hydrogel composite prepared by vapor deposition. (a) The composite in the shrunken (water-free) state. (b) A cross-section of the composite in the swollen state.

The "stamp" used in this synthesis is not a true stamp, since it contains no backing surface to which the raised surfaces are attached. When traditional stamps constructed from PDMS with similar patterns of ridges were used, no polyaniline formed on the poly(NIPAAm) surfaces located under the entire area occluded by the stamp. It can be observed from the pattern of polyaniline formation that polyaniline forms preferentially at the areas with the most surface area exposed to aniline vapor (the top corners, followed by the top edges).

Excitingly, samples prepared in this fashion exhibited higher conductivities when measurement probes were placed along a polyaniline pathway and lower conductivities when measurement probes were placed perpendicular to the pattern. As may be expected, electron transport occurs preferentially along the conductive polyaniline as opposed to the insulating poly(NIPAAm). Theoretically, the patterns produced by this method could

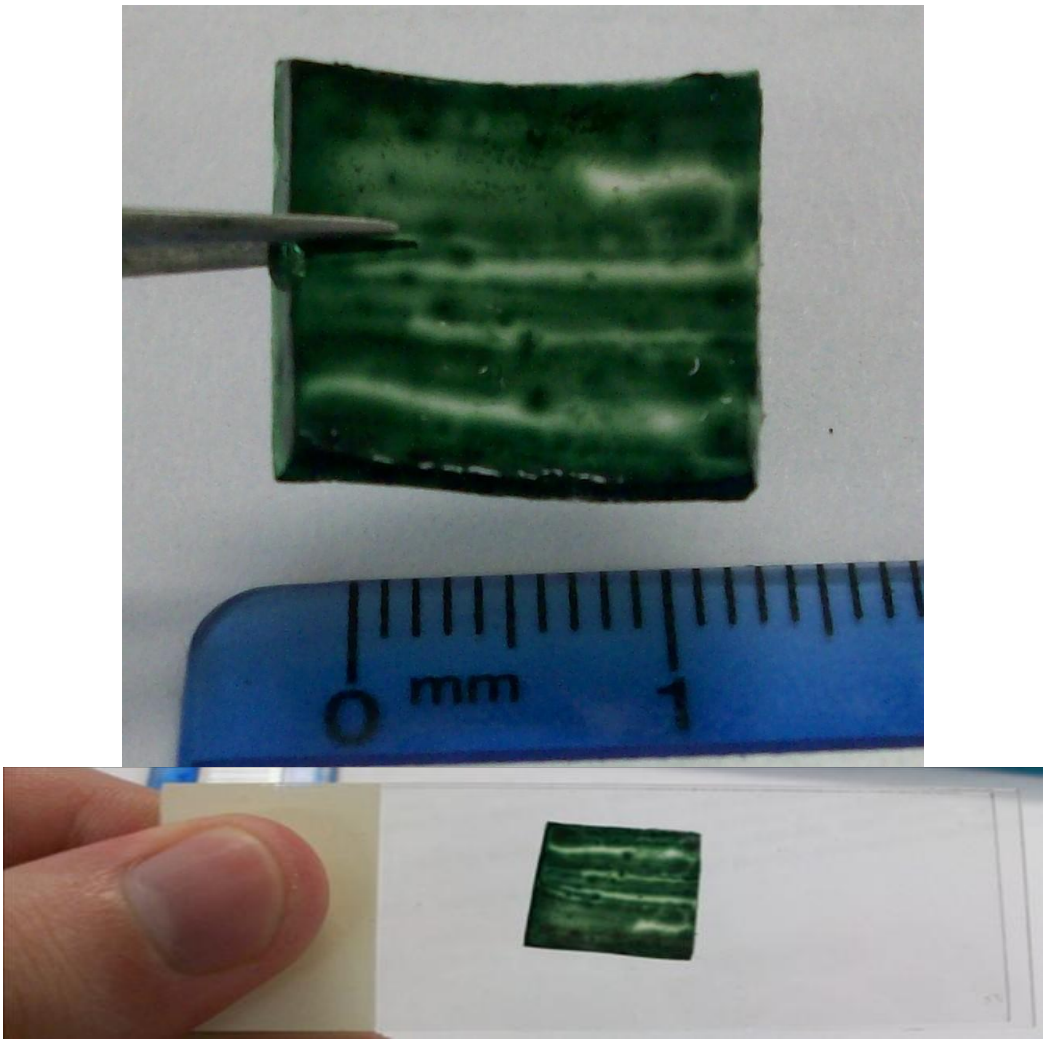

Figure 20. Photographs of the patterned polyaniline hydrogel composite prepared by vapor deposition in the swollen state.

be on the order of microns or nanometers, as long as an appropriate technique for producing micro- or nano-scale stamps was used. Whitesides provides several methods for producing micro and nano-scale PDMS stamps [70-72]. The swelling ratio q was calculated to be 4.6 at 25°C, which is somewhat lower than the ~8 given for homo-poly(NIPAAm) in the literature [73]. The conductivity of the patterned samples was measured with electrodes parallel to, perpendicular to, and at a 45° angle to the polyaniline pathways. The results are summarized in Table 3.

Table 3. The conductivity of a patterned polyaniline-hydrogel composite prepared by vapor deposition, measured with electrodes in different configurations.

	Parallel to Pathways	45° Angle to Pathways	Perpendicular to Pathways
Resistance (kΩ)	100 – 150	200 – 250	300
Conductivity S/cm	$2.43 – 3.65 \times 10^{-6}$	$1.46 – 1.82 \times 10^{-6}$	1.22×10^{-6}

C. Liquid Deposition

In the second method, a thin layer of liquid aniline was used to "ink" a PDMS stamp, which could be used to create a pattern of polyaniline on the surface of the poly(NIPAAm) film. Conceivably, this stamp could be as complicated as needed, and the lower bound on its size scale is limited only by the method by which liquid aniline can be applied only to the raised parts of the stamp and by the diffusion length of polyaniline in the poly(NIPAAm) system. If too much aniline is used, or if the lines to be inked are too close together, polyaniline may "bleed" between them and ruin the patterning.

Simple patterns of lines were also created by this method. As proof of concept, a micropipette was used to simply draw lines onto the surface of the poly(NIPAAm) using liquid aniline. The dark green polyaniline formed only in the areas touched by the liquid aniline. In this method, penetration of the polyaniline into the poly(NIPAAm) network is much deeper (approximately 0.5 mm), presumably because the much larger amount of aniline used means that the concentration gradient involved is much larger.

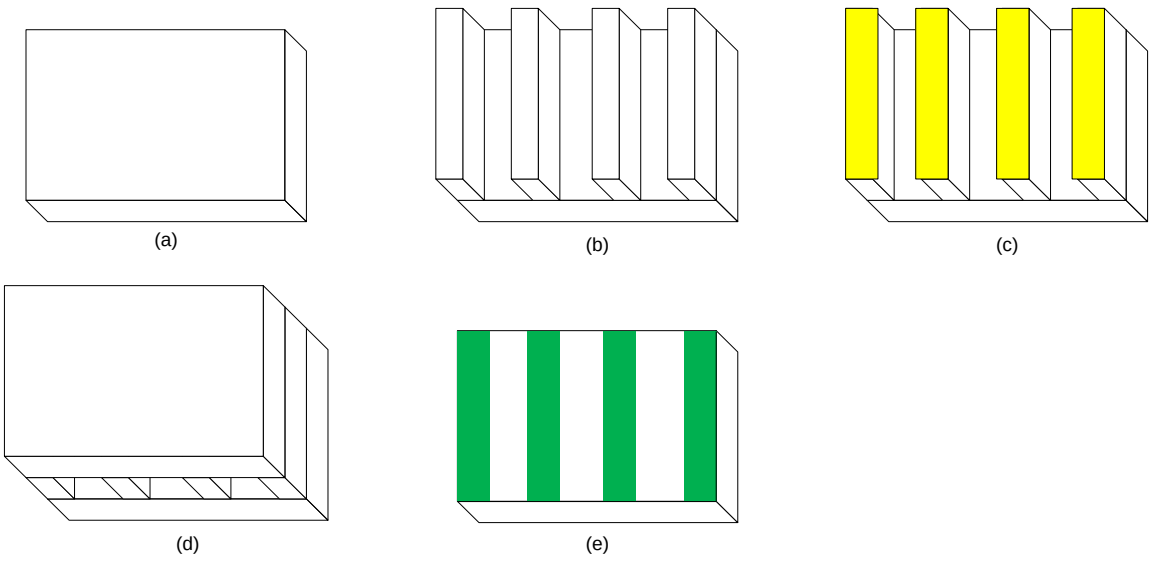

Figure 21. Surface polymerization of polyaniline onto a poly(NIPAAm) sample by template-assisted liquid deposition (dimensions have been exaggerated for clarity). (a) No exposure to aniline. (b) PDMS stamp is fabricated. (c) Liquid aniline is applied to raised areas of stamp. (d) Poly(NIPAAm) sample is placed on stamp. (e) PDMS stamp is removed, showing patterned polyaniline-hydrogel composite.

D. Considerations

It is important that the hydrogel soaking solution (1 M HCl, 0.1 M APS) is freshly prepared before polymerization is attempted. Ammonium persulfate begins to break down almost immediately when dissolved in water. If insufficient HCl remains in solution to dope the newly-forming polyaniline, it will polymerize in its de-doped dark blue emeraldine base phase [54]. This emeraldine base is extremely resistant to re-doping by HCl, possibly due to the interpenetration of polyaniline into the poly(NIPAAm) sample, which may prevent further movement of ions into the bulk polymer phase. If freshly polymerized samples are left in APS, even if any remaining surface aniline has been wiped free, further polymerization can occur with the remaining aniline which has diffused into the bulk poly(NIPAAm). This further polymerization can take the form of

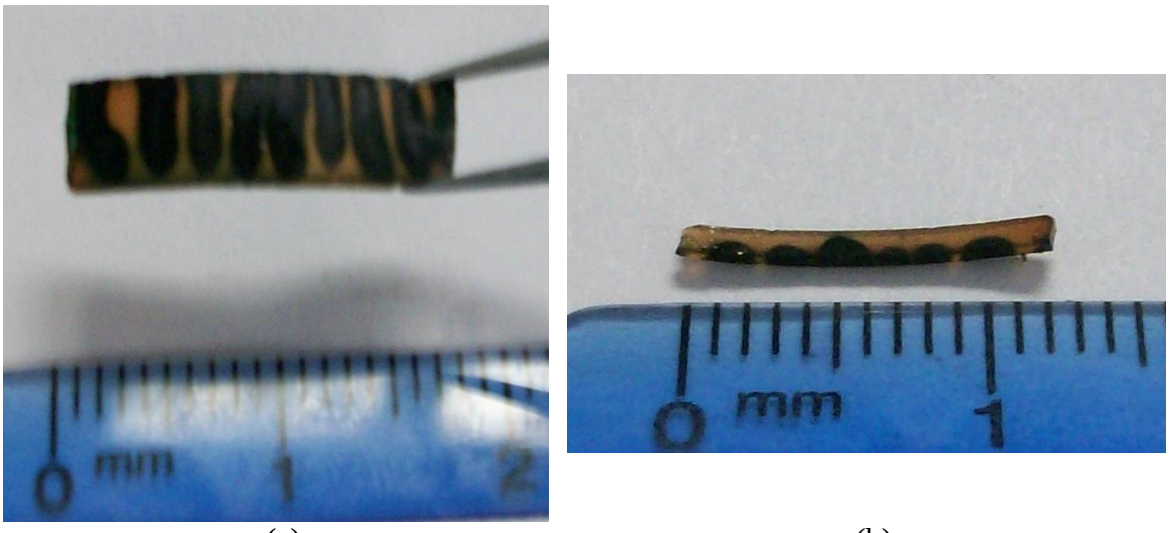

(a) (b)

Figure 22. Photographs of the patterned polyaniline hydrogel composite prepared by liquid deposition. (a) The composite in the swollen state. (b) A cross-section of the composite in the swollen state.

free polyaniline precipitating out the solution. If APS remains in the bulk poly(NIPAAm), the poly(NIPAAm) can turn reddish-brown after polymerization has occurred. This phenomenon is hypothesized to be either by the degradation of APS trapped in the bulk polymer sample or the formation of aniline oligomers which have a reddish-brown color [55]. Theoretically, this surface polymerization method can be extended to any hydrogel which is able to take up and hold the APS and HCl ions.

The amount of polyaniline which can be deposited onto the surface of the poly(NIPAAm) sample is limited by the amount of moisture in the hydrogel. If the poly(NIPAAm) remains open to the air for a long enough period of time (more than 24 hours), it will dry out, causing it to yellow and crack, and rendering it useless. This problem can be mitigated somewhat by ensuring that the reaction vessel is completely sealed. The sample will also crack if too much pressure is applied to it, as was often the case when weights were applied to the PDMS stamp in order to increase surface contact.

Instead, it is better to allow the surfaces to adhere themselves naturally. It is hypothesized that this contact is improved by the thin film of water remaining on the surface of the hydrogel sample.

IV. CONCLUSIONS

In this work, the synthesis and properties of a novel polyaniline-poly(NIPAAm) composite by vapor and liquid deposition showing directional conductivity have been described. This composite shows exciting properties and was prepared by methods as of yet unreported in the literature as far as our group is aware. The initiator and doping agent are introduced into the hydrogel by dissolving them in water and allowing them to be absorbed into the gel. Polyaniline layers can be formed on the surface of the hydrogel via a surface polymerization with the introduction of aniline either through direct contact in the liquid phase or in the vapor phase. PDMS stamps can be used to selectively block areas of the poly(NIPAAm) surface to create patterned polyaniline. This patterned composite shows directional conductivity in randomly-oriented polyaniline chains. This synthesis technique provides a low-cost, facile, and customizable method to develop a composite gel with exciting properties for the creation of artificial muscles using readily available and comparatively non-toxic materials.

V. FURTHER WORK & RECOMMENDATIONS

To ensure its viability as electroactive elements, the electrical properties of the composite need to be more adequately described. Only cursory measurements of conductivity were taken, and only at one set of conditions. The response of the composite to electrical stimuli will need to be studied more in depth to include such factors as response time and the direction and extent of motion. If the composite is to be implanted in the body, measurements will need to be taken at conditions representative of the human body. If the electrical properties of the composite are found to be inadequate, gold nanoparticles, such as spheres, rods, or wires, could be used to increase the conductivity.

Theoretically, there is no lower limit on the size scale of the patterning which could be achieved using this method except for the lateral diffusion length of polyaniline, which would cause the patterned areas to bleed together. Soft lithographic techniques, such as micro-contact printing (μCP) [72] and dip-pen nanolithography (DPN) [71], could be used to scale down the dimensions of the polyaniline deposited on the surface of the composite. Unaltered PDMS is sufficiently hydrophilic to cause "beading" of liquid aniline placed on the surface of the stamp. If the surface of the PDMS stamp was altered by the addition of hydrophobic functional groups, a monolayer of aniline molecules could be created, which would evenly travel into the hydrogel by diffusion.

If the material is ultimately to be implanted in the body, as for a left ventricular assist device for the treatment of congestive heart failure, *in vitro* and *in vivo* studies of the material will need to be conducted to assess the risk factors involved. If the oligomers and salts remaining in the polymer matrix can be removed without affecting the

conductivity of the device, these studies should be fairly uneventful, as polyaniline and poly(NIPAAm) have both been used in biomedical applications previously.

VI. REFERENCES

1. Bar-Cohen, Y., *Electroactive polymers as artificial muscles: A review.* Journal of Spacecraft and Rockets, 2002. **39**(6): p. 822-827.
2. Calvert, P., *Polymer Gel Actuators: Fundamentals*, in *Biomedical Applications of Electroactive Polymer Actuators*, E.S. Federico Carpi, Editor. 2009. p. 7-41.
3. Vinogradov, A.M. *Accomplishments and future trends in the field of electroactive polymers*. 2008: SPIE.
4. Bar-Cohen, Y., *Current and future developments in artificial muscles using electroactive polymers.* Expert Review of Medical Devices, 2005. **2**(6): p. 731-740.
5. Guimard, N.K., N. Gomez, and C.E. Schmidt, *Conducting polymers in biomedical engineering.* Progress in Polymer Science, 2007. **32**(8-9): p. 876-921.
6. Bag, D.S. and K.U.B. Rao, *Smart polymers and their applications.* Journal of Polymer Materials, 2006. **23**(3): p. 225-248.
7. Wikipedia Contributors. *Four-terminal sensing*. Wikipedia, the Free Encyclopedia [cited 2010 April 4]; Available from: http://en.wikipedia.org/w/index.php?title=Four-terminal_sensing&oldid=351127877.
8. Bar-Cohen, Y. and Q.M. Zhang, *Electroactive polymer actuators and sensors.* Mrs Bulletin, 2008. **33**(3): p. 173-181.
9. Bar-Cohen, Y., *Biomimetics using electroactive polymers (EAP) as artificial muscles - A review.* Journal of Advanced Materials, 2006. **38**(4): p. 3-9.
10. Lange, U., N.V. Roznyatouskaya, and V.M. Mirsky, *Conducting polymers in chemical sensors and arrays.* Analytica Chimica Acta, 2008. **614**(1): p. 1-26.
11. Wikipedia Contributors. *Voltammetry*. Wikipedia, the Free Encyclopedia [cited 2010 April 21]; Available from: http://en.wikipedia.org/w/index.php?title=Voltammetry&oldid=337614586.
12. Mallikarjuna, N.N., et al. (2005) *Novel high dielectric constant nanocomposites of polyaniline dispersed with gamma-Fe_{<FONT SIZE='-1'>2</FONT>}O_{<FONT SIZE='-1'>3</FONT>} nanoparticles*. Journal of Applied Polymer Science, 1868-1874 DOI: 10.1002/app.21405.
13. Matsuguchi, M., et al., *Effect of NH3 gas on the electrical conductivity of polyaniline blend films.* Synthetic Metals, 2002. **128**(1): p. 15-19.
14. Racicot, R., et al. *Thin Film Conductive Polymers on Aluminum Surfaces: Interfacial Charge-Transfer and Anti-Corrosion Aspects*. in *SPIE*. 1995.
15. Artificial Muscle Inc. *Artificial Muscle Introduces World's First Line of Standard Electroactive Polymer (EAP) Linear Actuators*. 2006 [cited 2010 April 8]; Available from: http://www.ngenpartners.com/Files/Press%20Releases/AMI12506.pdf.
16. Rajan, M. *Electro-active Polymer Actuators To See Large Growth Rates*. 2009 [cited 2010 April 8]; Available from: http://www.prlog.org/10288194-electroactive-polymer-actuators-to-see-large-growth-rates.html.
17. Mallick, K., M.J. Witcomb, and M.S. Scurrell, *Gold in Polyaniline: Recent Trends.* Gold Bulletin, 2006. **39**: p. 166-174.
18. Huang, J., *Syntheses and applications of conducting polymer polyaniline nanofibers.* Pure and Applied Chemistry, 2006. **78**(1): p. 15-27.
19. Herod, T.E. and J.B. Schlenoff, *Doping-induced strain in polyaniline: stretchoelectrochemistry.* Chemistry of Materials, 1993. **5**(7): p. 951-955.
20. Huang, J., et al., *Nanostructured Polyaniline Sensors.* Chemistry - A European Journal, 2004. **10**(6): p. 1314-1319.

21. Kang, E.T., K.G. Neoh, and K.L. Tan, *Polyaniline: A polymer with many interesting intrinsic redox states.* Progress in Polymer Science, 1998. **23**(2): p. 277-324.
22. Kaneto, K., et al., *"Artificial muscle": Electromechanical actuators using polyaniline films.* Synthetic Metals, 1995. **71**(1-3): p. 2211-2212.
23. Neelgund, G.M., et al., *Synthesis and characterization of polyaniline derivative and silver nanoparticle composites.* Polymer International, 2008. **57**(10): p. 1083-1089.
24. Cho, S.H. and S.M. Park, *Electrochemistry of conductive polymers 39. Contacts between conducting polymers and noble metal nanoparticles studied by current-sensing atomic force microscopy.* Journal of Physical Chemistry B, 2006. **110**(51): p. 25656-25664.
25. Pandey, P.K., P. Smitha, and N.S. Gajbhiye, *Synthesis and characterization of nanostructured PZT encapsulated PVA-PAA hydrogel.* Journal of Polymer Research, 2008. **15**(5): p. 397-402.
26. IARC. *IARC Summary & Evaluation, Supplement 7, 1987*. 1987 [cited 2010 April 4]; Available from: http://www.inchem.org/documents/iarc/suppl7/aniline.html.
27. EPA. *Aniline (CASRN 62-53-3)* 2002 [cited 2010 April 4]; Available from: http://www.epa.gov/iris/subst/0350.htm.
28. Wang, C.H., et al., *In-vivo tissue response to polyaniline.* Synthetic Metals, 1999. **102**(1-3): p. 1313-1314.
29. Granot, E., et al., *Enhanced bioelectrocatalysis using Au-nanoparticle/polyaniline hybrid systems in thin films and microstructured rods assembled on electrodes.* Chemistry of Materials, 2005. **17**(18): p. 4600-4609.
30. Jana, S., et al., *Effects of gold nanoparticles and lithium hexafluorophosphate on the electrical conductivity of PMMA.* Solid State Ionics, 2007. **178**(19-20): p. 1180-1186.
31. Tseng, R.J., et al., *Polyaniline Nanofiber/Gold Nanoparticle Nonvolatile Memory.* Nano Letters, 2005. **5**(6): p. 1077-1080.
32. Mallick, K., M.J. Witcomb, and M.S. Scurrell, *Polyaniline stabilized highly dispersed gold nanoparticle: an in-situ chemical synthesis route.* Journal of Materials Science, 2006. **41**(18): p. 6189-6192.
33. Peppas, N.A., et al., *Hydrogels in Biology and Medicine: From Molecular Principles to Bionanotechnology.* Advanced Materials, 2006. **18**(11): p. 1345-1360.
34. Hüther, A. and G. Maurer, *Swelling of N-isopropyl acrylamide hydrogels in aqueous solutions of poly(ethylene glycol).* Fluid Phase Equilibria 2004. **226**: p. 321-332.
35. Kumar, A., et al., *Synthesis and characterization of pH sensitive poly(PEGDMA-MAA) copolymeric microparticles for oral insulin delivery.* Journal of Applied Polymer Science, 2008. **107**(2): p. 863-871.
36. Satarkar, N.S. and J.Z. Hilt, *Hydrogel nanocomposites as remote-controlled biomaterials.* Acta Biomaterialia, 2008. **4**(1): p. 11-16.
37. Nandi, S. and H.H. Winter, *Swelling Behavior of Partially Cross-Linked Polymers: A Ternary System.* Macromolecules, 2005. **38**(10): p. 4447-4455.
38. Maurer, G. and J.M. Prausnitz, *Thermodynamics of phase equilibrium for systems containing gels.* Fluid Phase Equilibria 1996. **115**: p. 113-133.
39. Wang, J.H., *Self-Diffusion Coefficients of Water.* The Journal of Physical Chemistry, 1965. **69**(12): p. 4412-4412.
40. Ravve, A., *Light-Associated Reactions of Synthetic Polymers*. 2006: Springer.
41. Osswald, T.A. and G. Menges, *Materials Science of Polymers for Engineers*. 2 ed. 2003: Hanser.
42. Okay, O., *Macroporous Hydrogels from Smart Polymers*, in *Smart Polymers*, I. Galaev and B. Mattiasson, Editors. 2007, CRC Press. p. 269-293.

43. Bassil, M., J. Davenas, and M. El Tahchi, *Electrochemical properties and actuation mechanisms of polyacrylamide hydrogel for artificial muscle application.* Sensors and Actuators B-Chemical, 2008. **134**(2): p. 496-501.
44. Aouada, F.A., et al., *PAAm and PEDOT/PSS hydrogel as potential electroactive devices: evaluation of surface and hydrophilic properties.* E-Polymers, 2008.
45. Jianqi, F. and G. Lixia, *PVA/PAA thermo-crosslinking hydrogel fiber: preparation and pH-sensitive properties in electrolyte solution.* European Polymer Journal, 2002. **38**(8): p. 1653-1658.
46. Kim, S.J., et al., *Electroactive characteristics of interpenetrating polymer network hydrogels composed of poly(vinyl alcohol) and poly(N-isopropylacrylamide).* Journal of Applied Polymer Science, 2003. **89**(4): p. 890-894.
47. Shang, J., Z.Z. Shao, and X. Chen, *Chitosan-based electroactive hydrogel.* Polymer, 2008. **49**(25): p. 5520-5525.
48. Shim, W.S. and D.S. Lee, *Electroactive and temperature-sensitive hydrogel composites.* Journal of Applied Polymer Science, 1999. **74**(2): p. 311-321.
49. Vu, Y.-q., et al., *Synthesis and characterization of thermoresponsive hydrogels cross-linked with acryloyloxyethylaminopolysuccinimide.* Colloid and Polymer Science, 2007. **285**: p. 1553-1560.
50. McFarland, A.D., et al., *Color My Nanoworld.* Journal of Chemical Education, 2004. **81**(4): p. 544A.
51. Jana, N.R., L. Gearheart, and C.J. Murphy, *Wet chemical synthesis of high aspect ratio cylindrical gold nanorods.* Journal of Physical Chemistry B, 2001. **105**(19): p. 4065-4067.
52. Gao, J.X., C.M. Bender, and C.J. Murphy, *Dependence of the gold nanorod aspect ratio on the nature of the directing surfactant in aqueous solution.* Langmuir, 2003. **19**(21): p. 9065-9070.
53. Satarkar, N.S. and J.Z. Hilt, *Magnetic hydrogel nanocomposites for remote controlled pulsatile drug release.* Journal of Controlled Release, 2008. **130**(3): p. 246-251.
54. Huang, J., et al., *Polyaniline Nanofibers: Facile Synthesis and Chemical Sensors.* Journal of the American Chemical Society, 2002. **125**(2): p. 314-315.
55. Wang, J.X., et al., *Assembly of polyaniline nanostructures.* Macromolecular Rapid Communications, 2007. **28**(1): p. 84-87.
56. Li, X.G., A. Li, and M.R. Huang, *Facile High-Yield Synthesis of Polyaniline Nanosticks with Intrinsic Stability and Electrical Conductivity.* Chemistry-a European Journal, 2008. **14**(33): p. 10309-10317.
57. Wang, Y., et al., *Facile synthesis of polyaniline nanofibers using chloroaurate acid as the oxidant.* Langmuir, 2005. **21**(3): p. 833-836.
58. Kinyanjui, J.M., et al., *Chemical Synthesis of a Polyaniline/Gold Composite Using Tetrachloroaurate.* Chemistry of Materials, 2004. **16**(17): p. 3390-3398.
59. Xiang, Q. and H.Q. Xie, *Preparation and characterization of alkali soluble polyacrylamide-g-polyaniline.* European Polymer Journal, 1996. **32**(7): p. 865-868.
60. Hu, H., et al., *Electrically Conducting Polyaniline-Poly(acrylic acid) Blends.* Polymer International, 1998. **45**(3): p. 262-270.
61. Mirmohseni, A. and G.G. Wallace, *Preparation and characterization of processable electroactive polyaniline-polyvinyl alcohol composite.* Polymer, 2003. **44**(12): p. 3523-3528.
62. Cao, Y., P. Smith, and A.J. Heeger, *Spectroscopic studies of polyaniline in solution and in spin-cast films.* Synthetic Metals, 1989. **32**(3): p. 263-281.

63. Athawale, A.A., M.V. Kulkarni, and V.V. Chabukswar, *Studies on chemically synthesized soluble acrylic acid doped polyaniline.* Materials Chemistry and Physics, 2002. **73**(1): p. 106-110.
64. Moharram, M.A., M.A. Soliman, and H.M. El-Gendy, *Electrical conductivity of poly(acrylic acid)-polyacrylamide complexes.* Journal of Applied Polymer Science, 1998. **68**(12): p. 2049-2055.
65. Sun, L., S.C. Yeang, and J.-M. Liu. *Conducting Polymer with Improved Long-Time Stability: Polyaniline-Polyelectrolyte Complex*. in *Materials Research Society Symposium*. 1994.
66. Das, B., et al., *Synthesis and characterization of polyacrylamide-polyaniline conductive blends.* Journal of Applied Polymer Science, 1998. **69**(5): p. 841-844.
67. Monkman, A.P. and P. Adams, *Optical and electronic properties of stretch-oriented solution-cast polyaniline films.* Synthetic Metals, 1991. **40**(1): p. 87-96.
68. Miller, L.L., C.J. Zhong, and P. Kasai, *Production of a polymer with highly anisotropic conductivity and structure by Co-electroprecipitation of an imide anion radical and polycation.* Journal of the American Chemical Society, 1993. **115**(14): p. 5982-5990.
69. Krinke, Thomas J., et al., *Nanostructured Deposition of Nanoparticles from the Gas Phase.* Particle & Particle Systems Characterization, 2002. **19**(5): p. 321-326.
70. Bowden, N., et al., *Spontaneous formation of ordered structures in thin films of metals supported on an elastomeric polymer.* Nature, 1998. **393**(6681): p. 146-149.
71. Kumar, A., H.A. Biebuyck, and G.M. Whitesides, *Patterning Self-Assembled Monolayers - Applications in Materials Science.* Langmuir, 1994. **10**(5): p. 1498-1511.
72. Xia, Y. and G.M. Whitesides, *Soft Lithography.* Annual Review of Materials Science, 1998. **28**(1): p. 153-184.
73. Bae, Y.H., T. Okano, and S.W. Kim, *"On–Off" Thermocontrol of Solute Transport. I. Temperature Dependence of Swelling of N-Isopropylacrylamide Networks Modified with Hydrophobic Components in Water.* Pharmaceutical Research, 1991. **8**(4): p. 531-537.
74. Winter, E.M. and F.B.C. Brooks, *Electromechanical response times and muscle elasticity in men and women*. European Journal of Applied Physiology and Occupational Physiology, 1991. **63**(2): p. 124-128.

VITA

Eric Reed was born January 16, 1987 in Detroit, Michigan, but has resided for most of his life in Franklin, Tennessee. He attended Christ Presbyterian Academy in Nashville, Tennessee and graduated Co-Salutatorian of his class in 2005.

Eric began attending the University of Louisville in 2005. He played alto saxophone for three years in the University of Louisville Marching Band, and graduated with honors with his Bachelor of Science in Chemical Engineering in December 2009. He will graduate with his Master of Engineering in Chemical Engineering in May 2010. Eric plans to work in industry following his graduation.